Towards optimized suppression of dephasing in systems subject to pulse timing constraints

Thomas E. Hodgson,[1] Lorenza Viola,[2] and Irene D'Amico[1]

[1]*Department of Physics, University of York, Heslington, York YO10 5DD, United Kingdom*

[2]*Department of Physics and Astronomy, 6127 Wilder Laboratory, Dartmouth College, Hanover, New Hampshire 03755, USA*

We investigate the effectiveness of different dynamical decoupling protocols for storage of a single qubit in the presence of a purely dephasing bosonic bath, with emphasis on comparing quantum coherence preservation under uniform versus nonuniform delay times between pulses. In the limit of instantaneous bit-flip pulses, this is accomplished by establishing a different representation of the controlled qubit evolution, where the decoherence behavior after an arbitrary number of pulses is directly expressed in terms of the uncontrolled decoherence function. In particular, analytical expressions are obtained for approximation of the long- and short-term coherence behavior for both Ohmic and supra-Ohmic environments. By focusing on the realistic case of pure dephasing in an excitonic qubit, we quantitatively assess the impact of physical constraints on achievable pulse separations, and show that little advantage of high-level decoupling schemes based on concatenated or optimal design may be expected if pulses cannot be applied sufficiently fast. In such constrained scenarios, we demonstrate how simple modifications of repeated periodic-echo protocols can offer significantly improved coherence preservation in realistic parameter regimes. We expect similar conclusions to be relevant to other constrained qubit devices exposed to quantum or classical phase noise.

I. INTRODUCTION

The ability to effectively counteract decoherence processes in physical quantum-information processing (QIP) devices is a fundamental prerequisite for taking advantage of the extra power promised by quantum computation and quantum simulation as compared to purely classical approaches. Dynamical decoupling (DD) techniques for open quantum systems [1,2] have been shown to be able to significantly suppress non-Markovian decoherence for storage times that can be very long relative to the typical time scales associated with the decoherence process itself. Physically, DD borrows inspiration from the idea of *coherent averaging* of unwanted interactions, as pioneered in the nuclear magnetic resonance (NMR) community following the landmark discovery of the spin-echo effect [3] and its extension to a variety of multiple-pulse sequences elegantly designed based on so-called average Hamiltonian theory by Haeberlen and Waugh [4–6].

Prompted by the unprecedented level of coherent control demanded by QIP applications, the design and characterization of viable DD schemes for realistic qubit systems has spurred an intense theoretical and experimental effort over the last decade, taking DD well beyond its traditional boundaries. While earlier DD schemes relied on the simple periodic repetition of instantaneous pulses [so-called "bang-bang" periodic DD (PDD) [2], and its closely related time-symmetrized version, the so-called Carr-Purcell DD (CPDD) [5,7]], subsequent theoretical investigations have explored the benefits of more sophisticated control design in a number of ways. On the one hand, this has led to extending a number of NMR-inspired design principles for pulse sequences within a general open-system framework, and to rigorously assessing their performance—most notably, recursive "supercycle" techniques from NMR [4] have been incorporated in "concatenated" DD (CDD) protocols for generic decoherence models on finite-dimensional quantum systems [8,9]. On the other hand, qualitatively different approaches to synthesizing pulse sequences have also emerged,

including "randomized" DD schemes [10,11], that attempt to optimize control performance in a suitable average sense, as well as "optimal" approaches that directly minimize the decoherence error in specific control scenarios under various assumptions. Prominent examples are so-called Uhrig DD (UDD) for a single qubit undergoing pure dephasing (pure T_2 decoherence) [12–17], and its extension to "locally optimized" [18,19] DD sequences tailored to specific noise environments; and, most recently, protocols that combine the advantages of concatenation and optimization for a single qubit exposed to arbitrary (both T_2 and T_1) decoherence [20–22]. As a key common feature, these investigations highlight the sensitivity of DD performance to the details of the applied control protocol, and point to the importance of careful tuning of the *pulse timings* in order to boost the efficiency of the achievable decoherence suppression [23].

In view of the above rich scenario, assessment of the performance of different DD protocols in specific qubit devices and/or in the presence of specific control constraints becomes especially important from an implementation perspective. In this context, the effectiveness of traditional multipulse spin-echo sequences based on PDD and CPDD, as compared to "high-level" protocols based on CDD and UDD, has been recently scrutinized in several control settings. In particular, a number of theoretical studies have addressed suppression of pure dephasing associated with spectral diffusion [25] and hyperfine-induced decoherence [26] from a quantum spin bath for an electron spin qubit, as well as suppression of classical $1/f$ phase noise in a superconducting qubit [27,28]. Experimentally, the performance of CDD protocols has been characterized for an NMR spin qubit [29], while UDD implementations have been reported for both trapped ion qubits exposed to engineered classical phase noise [18,19,30] and, in the solid state, for electron spin qubits undergoing spin-bath decoherence in a malonic acid crystal [31]. Interestingly, beyond the QIP setting, the use of highly nonuniform UDD

pulse timings has also recently proved to yield enhanced refocusing and contrast in magnetic resonance imaging of certain structured samples such as tissue [32]. Overall, these studies have demonstrated how UDD can significantly outperform low-level DD schemes provided that the noise spectrum has a "hard" high-frequency cutoff and sufficiently high pulse repetition rates may be afforded.

Among prospective solid-state QIP platforms, exciton qubits in self-assembled quantum dots (QDs) have likewise received much attention in recent years [33,34]: because of the coupling to photons, excitons can be driven all-optically on subpicosecond time scales [33], while allowing for flexibility in designing hybrid solid state-flying qubit schemes [35,36]. As a down side, pure dephasing severely limits the coherence lifetime in such qubit devices, where strong coupling with phonon modes of the host crystal results in typical decoherence (T_2) time scales of a few picoseconds [37]. We have previously shown in Ref. [38] that, remarkably, PDD allows for substantial exciton coherence recovery in experimentally relevant parameter regimes (up to 90% recovery over ∼10 ps at room temperature), the control performance being especially enhanced for QD shapes and bias fields optimized for quantum-computing architectures. Motivated by these results, our main goal in this paper is to quantitatively assess to what extent more elaborated DD schemes—in particular, sequences employing nonuniform pulse timings—can further improve beyond the simplest PDD setting while respecting the *lower bound on the achievable control time scale* (minimum pulse separation) that is intrinsic to the system.

Our analysis shows that, in the presence of such a timing limitation, elementary protocols such as PDD or CPDD outperform high-level sequences based on CDD or UDD. While degradation of UDD performance for "soft" spectral cutoffs is expected theoretically [15] (see also [40] for a recent related experiment), our results on the implications of *timing restrictions* reinforce and extend earlier conclusions drawn in Ref. [28] for classical dephasing in superconducting qubits. In addition, we explicitly show how it is possible to engineer a suitable "preparatory" sequence that enhances the performance of a subsequent PDD pulse train while taking the relevant timing constraint into account. In the process, we take advantage of the exact solvability of a purely dephasing model in the presence of instantaneous pulses to obtain an exact representation of the controlled decoherence function in terms of its free (uncontrolled) counterpart. This allows rigorous results on the long-time asymptotic decoherence behavior to be established for generic noise spectral densities, by allowing, in particular, a direct comparison between Ohmic and supra-Ohmic environments. Furthermore, our work provides an explicit analysis of CDD in the presence of a quantum bosonic bath, complementing existing studies for quantum spin baths [9,25,26,29] or semiclassical environments [28] (see also Ref. [39] for recent rigorous performance bounds).

From a practical standpoint, our results suggest that periodic control protocols such as CPDD (or simple modifications thereof) might remain a method of choice if significant timing constraints are in place, and that incorporation of such constraints *from the outset* is necessary before further optimization can show its benefits. While our numerical results

are tailored, as mentioned, to excitons in QDs, we note that our derivation also applies, with minor modifications, to a qubit subject to classical (Gaussian) phase noise. Thus, we expect that our conclusions may be of direct relevance to other noisy qubit devices in *constrained parameter regimes*, including, for instance, trapped-ion qubits [18,19] and trapped atomic ensembles [40], superconducting qubits exposed to charge or flux noise [28,41], as well as semiconductor spin qubits affected by charge noise [42].

II. SINGLE-QUBIT DEPHASING DYNAMICS

A. Noise model

We focus on the pure dephasing dynamics of a single qubit coupled to a noninteracting quantum bath of harmonic oscillators. In the absence of external control, the joint Hamiltonian of such a system may be written in the form

$$H = \frac{E}{2}\sigma_z + \hbar \sum_j \omega_j b_j^\dagger b_j + \hbar \sum_j (g_j^* b_j^\dagger + g_j b_j)$$
$$\times [(1-\alpha)\sigma_0 + \alpha\sigma_z] \qquad (1)$$

$$\equiv H_0 + \hbar \sum_j (g_j^* b_j^\dagger + g_j b_j)[(1-\alpha)\sigma_0 + \alpha\sigma_z], \qquad (2)$$

where E gives the energy difference between the qubit's levels, σ_z and σ_0 denote Pauli operators (with σ_0 being the identity), $b_j^\dagger$ and b_j are canonical creation and annihilation operators of the jth oscillator mode, and g_j describes the coupling between the qubit and the jth bath mode. In this expression for H, the parameter α accounts for the possibility that either both or only one of the spin (or pseudospin) qubit computational levels effectively couple to the bath: $\alpha = 1$ corresponds to the standard purely dephasing spin-boson model, whereas if $\alpha = 1/2$, only the $\sigma_z = +1$ eigenstate couples to the bath. This is the case for an excitonic qubit, where the logical states are represented by the presence or absence of a single (ground-state) exciton in the QD [33], and E is the energy relative to the crystal ground state.

As time evolves, the qubit becomes entangled with the environment, and the off-diagonal elements of the qubit density matrix evaluated at time t in the interaction picture with respect to H_0 read [1,37,43,44]

$$\rho_{01}(t) = \rho_{10}^*(t) = \rho_{01}(t=0)e^{-\Gamma_0(t)}, \qquad (3)$$

$$\Gamma_0(t) = (2\alpha)^2 \int_0^\infty \frac{I(\omega)}{\omega^2} \coth\left(\frac{\hbar\omega}{2k_B T}\right)[1 - \cos(\omega t)]d\omega, \qquad (4)$$

where T is the temperature, k_B Boltzmann's constant, and

$$I(\omega) = \sum_j \delta(\omega - \omega_j)|g_j|^2$$

is the spectral density function characterizing the interaction of the qubit with the oscillator bath. For a supra-Ohmic environment, $I(\omega) \overset{\omega\to 0}{\sim} \omega^3$, as opposed, for instance, to an Ohmic reservoir where $I(\omega) \overset{\omega\to 0}{\sim} \omega$. Likewise, the high-frequency behavior is characterized by a frequency cutoff ω_c, $I(\omega) \overset{\omega\to\infty}{\sim} f(\omega,\omega_c)$, for a function f that decays to zero

sufficiently fast for $\omega > \omega_c$. For excitons, as we shall see, $f(\omega, \omega_c) \sim e^{-\omega^2/\omega_c^2}$.

Our analysis takes advantage of the fact that the decoherence of the qubit in the presence of an *arbitrary* sequence of bang-bang pulses, each effecting an instantaneous π rotation, can still be exactly described by Eq. (3), provided a modified decoherence function Γ—instead of Γ_0—is used [2,13,45]. Consider an arbitrary storage time t, during which a total number s of pulses is applied, at instants $\{t_1, \ldots, t_n, \ldots, t_s\}$, with $0 < t_1 < t_2 < \cdots < t_s < t$. By using the theory developed by Uhrig in Refs. [13,14], a controlled coherence function $\Gamma(t)$ can be defined as follows:

$$\Gamma(t) \equiv \begin{cases} \Gamma_0(t), & t \leqslant t_1, \\ \Gamma_n(t), & t_n < t \leqslant t_{n+1}, \quad 0 < n < s, \\ \Gamma_s(t), & t_s < t. \end{cases} \quad (5)$$

Here, $\Gamma_0(t)$ is given in Eq. (4) and, for $1 \leqslant n \leqslant s$,

$$\Gamma_n(t) = (2\alpha)^2 \int_0^\infty \frac{I(\omega)}{2\omega^2} \coth\left(\frac{\hbar\omega}{2k_B T}\right) |y_n(\omega t)|^2 d\omega,$$

$$y_n(z) = 1 + (-1)^{n+1} e^{iz} + 2\sum_{m=1}^n (-1)^m e^{iz\delta_m}, \quad z > 0,$$

with the nth pulse being understood to occur at time $t_n = \delta_n t$, and $0 < \delta_1 < \cdots < \delta_n < \cdots < \delta_s < 1$. The controlled decoherence function $\Gamma(t)$ may be compactly rewritten as

$$\Gamma(t) \equiv \Gamma_n(t) = \int_0^\infty \eta(\omega)|y_n(\omega t)|^2 d\omega, \quad n \geqslant 0, \quad (6)$$

with the definitions

$$|y_0(\omega t)|^2 \equiv |1 - e^{i\omega t}|^2 \quad (7)$$

and

$$\eta(\omega) = (2\alpha)^2 \frac{I(\omega)}{2\omega^2} \coth\left(\frac{\hbar\omega}{2k_B T}\right). \quad (8)$$

Remarkably, it turns out that the dephasing dynamics in the presence of control can be *entirely* expressed in terms of the free dephasing dynamics, for arbitrary n. First, notice that by relating $|y_1(\omega t)|^2$ to $|y_0(\omega t)|^2$ we may write

$$\Gamma_1(t) = -\Gamma_0(t) + 2\Gamma_0(t_1) + 2\Gamma_0(t - t_1). \quad (9)$$

Upon continuation of this iteration, this yields

$$\Gamma_2(t) = -\Gamma_1(t) + 2\Gamma_1(t_2) + 2\Gamma_0(t - t_1),$$
$$\vdots \quad (10)$$
$$\Gamma_n(t) = -\Gamma_{n-1}(t) + 2\Gamma_{n-1}(t_n) + 2\Gamma_0(t - t_n).$$

By relating, again, $|y_n(\omega t)|^2$ to $|y_0(\omega t)|^2$, we find the following exact expression:

$$\Gamma_n(t) = 2\sum_{m=1}^n (-1)^{m+1} \Gamma_0(t_m)$$

$$+ 4\sum_{m=2}^n \sum_{j<m} \Gamma_0(t_m - t_j)(-1)^{m-1+j}$$

$$+ 2\sum_{m=1}^n (-1)^{m+n} \Gamma_0(t - t_m) + (-1)^n \Gamma_0(t). \quad (11)$$

The above equation is one of the main results of this paper. By use of Eq. (11), it is, in particular, straightforward to see that

$$\Gamma_{n-1}(t_n) = \lim_{t \to t_n} \Gamma_n(t) = \Gamma_n(t_n). \quad (12)$$

This confirms that the function $\Gamma(t)$ as defined in Eq. (5) is continuous at the (instantaneous) pulse timings, as expected on physical grounds.

It is worth noting that a very similar derivation is applicable to pure dephasing dynamics arising from classical noise, as described by a model Hamiltonian of the form

$$H = \frac{1}{2}[E + \beta(t)]\sigma_z, \quad (13)$$

the function $\beta(t)$ representing a classical stochastic process. Provided that the statistics of the fluctuations is Gaussian, the noise is completely characterized by its power spectrum $S(\omega)$, which is determined by the two-point correlation noise function via

$$S(\omega) = \int_{-\infty}^\infty e^{i\omega t} S(t)dt, \quad S(t_2 - t_1) = \langle \beta(t_1)\beta(t_2)\rangle,$$

under the assumption that the ensemble average $\langle \beta(t)\rangle = 0$. The influence of the noise on the qubit-controlled dynamics is then evaluated through an average over all possible realizations, which leads to a decoherence function still formally given by Eq. (6), upon the replacement [27,28,43]

$$\eta(\omega) \mapsto \eta'(\omega) = \frac{1}{\pi} \frac{S(\omega)}{2\omega^2}. \quad (14)$$

Thus, while our emphasis in what follows will be on analyzing phase decoherence from a quantum bath, the exact representation established in Eq. (11) holds also for arbitrary Gaussian phase randomization processes, such as recently engineered, for instance, in experimental studies of UDD using trapped ions [18,19] or as naturally occurring in dense atomic ensembles [40] and in a variety of solid-state qubits [28,41,42].

As a first concrete example of the usefulness of the result in Eq. (11), we consider how two pulses may be used to increase the asymptotic coherence of a supra-Ohmic system, for which the free dephasing dynamics is known to saturate in the long-time limit to a *finite* value [37,43] $\Gamma_0(\infty) > 0$. Taking the $t \to \infty$ limit in Eq. (9) or, equivalently, letting $n = 1$ in Eq. (11), we get $\Gamma_1(\infty) = 2\Gamma_0(t_1) + \Gamma_0(\infty)$. Since $\Gamma_0(t) \geqslant 0$ for all t, this shows how a single pulse cannot decrease the asymptotic decoherence level. However, after two pulses we have

$$\Gamma_2(t) = \Gamma_0(t) - 2\Gamma_0(t - t_1) - 2\Gamma_0(t_2) + 2\Gamma_0(t_1)$$
$$+ 4\Gamma_0(t_2 - t_1) + 2\Gamma_0(t - t_2). \quad (15)$$

Therefore,

$$\Gamma_2(\infty) = \Gamma_0(\infty) - 2\Gamma_0(t_2) + 2\Gamma_0(t_1) + 4\Gamma_0(t_2 - t_1), \quad (16)$$

and t_1 and t_2 can be chosen to decrease the asymptotic decoherence provided that

$$\Gamma_0(t_2) - \Gamma_0(t_1) > 2\Gamma_0(t_2 - t_1). \quad (17)$$

The possibility of satisfying Eq. (17) as well as the significance of the general representation given in Eq. (11) will be explicitly illustrated in what follows.

B. Exciton qubit dephasing

The excitonic system of interest is discussed in detail in Ref. [38]. The relevant spectral density is given by

$$I(\omega) = I_e(\omega) + I_h(\omega) + I_{eh}(\omega), \tag{18}$$

where the indices e, h, and eh correspond to single-particle spectral densities of the electron and the hole, and to the electron-hole interference term, respectively, and

$$I_{e|h|eh}(\omega) = \sum_i F_i^{e|h|eh}(\omega) \exp\left(-\frac{\omega^2}{\omega_{c_i,e|h|eh}^2}\right). \tag{19}$$

Here, i labels different phonon modes, whereas $F_i^{e|h|eh}(\omega)$ is a mode-dependent function for which $F_i^{e|h|eh}(\omega) \overset{\omega \to 0}{\leqslant} \omega^3$. The spectral density may be further approximated as

$$I(\omega) \approx F\omega^3 \exp\left(-\frac{\omega^2}{\omega_c^2}\right), \tag{20}$$

where the parameters F and ω_c are determined from a fit to the actual exciton spectral density. For illustration purposes, all the numerical examples in this paper will consider (unless otherwise stated) an exciton qubit tightly confined within a GaAs QD at $T = 77$ K. The QD potentials are modeled as parabolic in all three dimensions, with confinement energies in the z direction of $\hbar\omega_e = 505$ meV and $\hbar\omega_h = 100$ meV, while $\hbar\omega_e = 30$ meV and $\hbar\omega_h = 24$ meV in the in-plane directions [33,47]. This also yields $F = 1.14 \times 10^{-26}$ s and $\hbar\omega_c = 2$ meV. Physically, the quantity $|\exp[-\Gamma(t)]|^2$ is directly proportional to the square modulus of the measured optical polarization $\mathbf{P}(t)$. In the absence of control, most of the coherence is typically lost after a few picoseconds [37,47].

The decoherence function $\Gamma(t)$ for an exciton qubit subject to two ideal control pulses at $t_1 = 0.2$ ps and $t_2 = 0.31$ ps is depicted in Fig. 1. While the instantaneous-pulse assumption must be handled with care in general, we have discussed in Ref. [38] how it translates into reasonable physical constraints for an excitonic qubit coupled to a phononic bath. For comparison, we also plot in the same figure the evolution under a single control pulse at $t_1 = 0.2$ ps, as well as the free evolution $\Gamma_0(t)$. As one can see, Eq. (17) can indeed be satisfied. Numerical results showing how a few pulses can increase the asymptotic
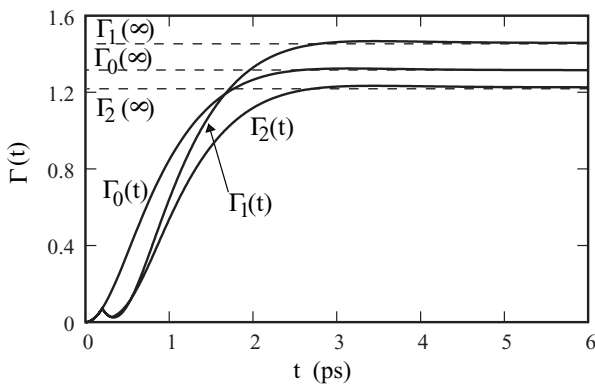
coherence have been reported for excitonic dephasing in Ref. [46].

III. PERIODIC DD: PERFORMANCE AND EXACT ASYMPTOTIC PROPERTIES

For a Hamiltonian as in Eq. (1), a DD cycle consisting of two uniformly spaced rotations by π about the x axis,

$$X\Delta t X\Delta t, \tag{21}$$

where time ordering is understood from right to left, removes the interaction between the qubit and the boson bath [2,9] to the lowest (perturbative) order in $\omega_c T_c$, with $T_c = 2\Delta t$. The simplest DD protocol, PDD, is obtained by iterating the above control cycle in time.

Figure 2 compares the free evolution with the PDD-controlled dephasing for the exciton qubit under examination, computed from the exact expressions given in Sec. II. Sequences with three different pulse delays are shown, $\Delta t = 0.1$, 0.2, and 0.3 ps, respectively. For the exciton qubit, two conditions determine a suitable range of Δt for effective PDD. On the one hand, it is necessary that the control time scale T_c be sufficiently short with respect to the (shortest) correlation time of the decoherence dynamics, which means in this case $2\Delta t \lesssim \tau_c = 2\pi/\omega_c$. Physically, this can also be interpreted by requiring that the characteristic frequency introduced by the periodic control,

$$\omega_{\text{res}} = \frac{\pi}{\Delta t},$$

be significantly higher than the spectral cutoff frequency itself, $\omega_{\text{res}} \gtrsim \omega_c$, in such a way that the DD-renormalized spectral density function $I(\omega) \tan^2(\omega\Delta t/2)$ is effectively upshifted beyond the bath cutoff [15,22,38,49]. The second condition derives from the existence of a lower bound on the pulse duration, which implies a lower bound on the separation Δt in order for the instantaneous-pulse description to be accurate. As discussed in Ref. [38], this means $\Delta t \gtrsim 0.1$ ps for semiconductor self-assembled QDs of interest for QIP.

The values of Δt used in Fig. 2, are consistent with both these conditions. It can be seen that coherence decays until the first bit flip occurs, after which it rises, reaches a local maximum before decohering once again, with this pattern
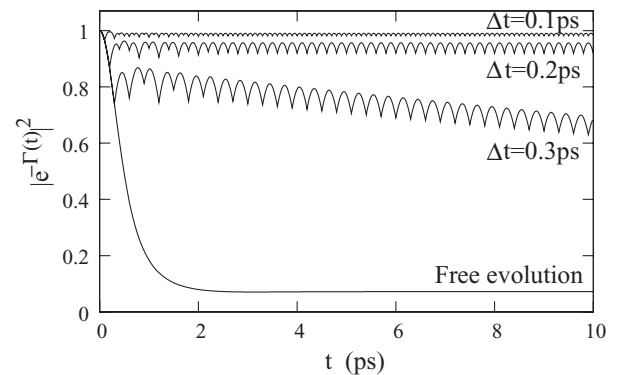
FIG. 1. Comparison between $\Gamma_0(t)$, $\Gamma_1(t)$, and $\Gamma_2(t)$ for an exciton qubit at $T = 77$ K, as computed from Eq. (5) (with $\alpha = 1/2$). Pulse times are $t_1 = 0.2$ ps and $t_2 = 0.31$ ps.

FIG. 2. $|\exp[-\Gamma(t)]|^2$ for the exciton qubit in the presence of PDD with $\Delta t = 0.1$, 0.2, and 0.3 ps, compared with the free evolution determined by $\Gamma_0(t)$.

repeating between every two bit flips. It can also be seen that DD recovers most of the dephasing, that is, $\exp[-\Gamma(t)]$ is much closer to unity than in the uncontrolled evolution, which falls rapidly before saturating to $\exp[-\Gamma_0(\infty)]$. After the first few initial pulses, the dephasing enters a phase in which the behavior after the $(n + 1)$th pulse is approximately the same as that after the nth pulse. For $\Delta t = 0.1$ and 0.2 ps, the average dephasing *over each cycle* in this "steady-state" phase is very small, leading to a practical "freezing" of the average decoherence over a period much longer than the estimated (subpicosecond) gating times [33]. For $\Delta t = 0.3$ ps, however, the increase of decoherence due to this average dephasing with time is more noticeable, leading to worse DD performance overall. It can also be seen that, to minimize the effects of dephasing, any readout on the qubit should be made halfway between two control pulses. As is well known in NMR, this motivates a proper choice of the observation window, which underlies the Carr-Purcell (CP) sequence [7] and is also discussed in Ref. [50] in the spin-boson context.

A. Long-time dynamics: Ohmic versus supra-Ohmic behavior

A main advantage of the exact representation established in Eq. (11) is that it allows detailed quantitative insight into the controlled dephasing behavior to be gained. In particular, we focus on long-time coherence properties, which have also received recent attention in view of control-dependent "saturation" effects observed in the context of spin-bath decoherence [51] (see also Ref. [52]). We start by quantifying how the decoherence function in the presence of n pulses differs between two consecutive control times. Let

$$\Delta\Gamma_n \equiv \Gamma_n(t_{n+1}) - \Gamma_{n-1}(t_n). \quad (22)$$

By using Eq. (11) we obtain

$$\Delta\Gamma_n = (-1)^n[\Gamma_0(t_{n+1}) - \Gamma_0(t_n)]$$
$$+ 2\sum_{j=1}^{n}\Gamma_0(t_{n+1} - t_j)(-1)^{n+j}$$
$$- 2\sum_{j=1}^{n-1}\Gamma_0(t_n - t_j)(-1)^{j+n}. \quad (23)$$

Let now $\Delta\Gamma_n^{\mathrm{PDD}}$ denote the "differential dephasing function" of Eq. (22), specialized to a PDD protocol. Then, as showed in Appendix A, the following asymptotic result holds for an *arbitrary dephasing environment*:

$$\Delta\Gamma_\infty \equiv \lim_{n\to\infty}\Delta\Gamma_n^{\mathrm{PDD}} = 8\omega_{\mathrm{res}}\eta(\omega_{\mathrm{res}}). \quad (24)$$

Interestingly, Eq. (24) can be used to describe how the dephasing function changes between *any* two instants separated by Δt, for large enough t. That is, consider

$$\Delta\Gamma_n^{\mathrm{PDD}}(\tilde{t}) \equiv \Gamma_{n+1}(\tilde{t} + t_{n+1}) - \Gamma_n(\tilde{t} + t_n), \quad (25)$$

where $0 \leqslant \tilde{t} \leqslant \Delta t$, $t_n = n\Delta t$. By using Eq. (12) we can verify that $\Delta\Gamma_n^{\mathrm{PDD}}(0) = \Delta\Gamma_n^{\mathrm{PDD}}$. Then one may also prove (see Appendix B for details) that

$$\Delta\Gamma_n^{\mathrm{PDD}}(\tilde{t}) \overset{n>n_{\mathrm{sat}}}{\approx} \Delta\Gamma_\infty, \quad (26)$$
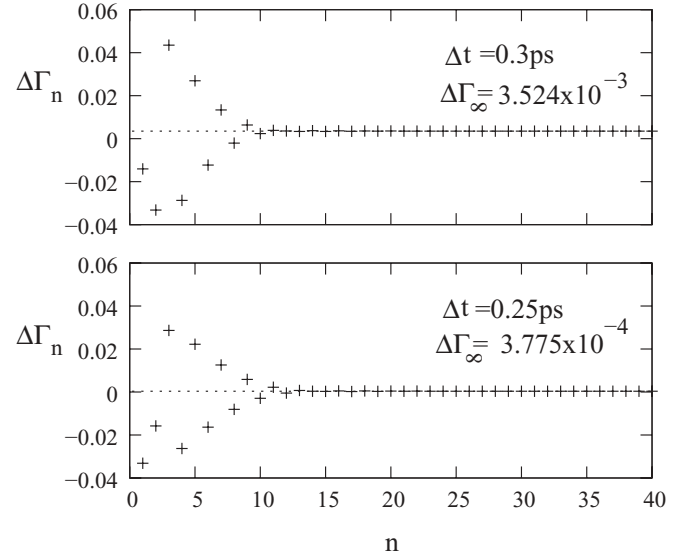

FIG. 3. Differential dephasing function, $\Delta\Gamma_n^{\mathrm{PDD}}$, for the exciton qubit under examination in the presence of PDD with $\Delta t = 0.3$ ps (top) and $\Delta t = 0.25$ ps (bottom), calculated from Eq. (23). The dotted lines show, in each case, the limiting value $\Delta\Gamma_\infty$ given by Eq. (24). Notice that for $n < n_{\mathrm{sat}}$, where $n_{\mathrm{sat}} \sim 15$, the sign of $\Delta\Gamma_n^{\mathrm{PDD}}$ oscillates, in agreement with Eqs. (B5) and (B7).

where $n_{\mathrm{sat}} \equiv t_{\mathrm{sat}}/\Delta t$ is a sufficiently large integer defined in the same Appendix. Equation (26) shows that the dephasing increment becomes *independent of n and $\tilde{t}$* for $t > t_{\mathrm{sat}}$, that is, dephasing asymptotically enters a periodic oscillation in phase with the PDD sequence. Thus, $\Delta\Gamma_\infty$ in Eq. (24) may be used to describe the difference in dephasing between any two times separated by Δt—in particular, between consecutive coherence maxima which for $t > t_{\mathrm{sat}}$ occurs at $\tilde{t} \approx \Delta t/2$. For a supra-Ohmic environment as in the exciton qubit, the convergence of $\Delta\Gamma_n^{\mathrm{PDD}}$ to $\Delta\Gamma_\infty$, Eq. (24), is very fast. This is illustrated in Fig. 3 for two representative values of Δt.

Because $\Delta\Gamma_\infty$ in Eq. (24) is nonzero as long as Δt is finite, we can infer that Γ_n diverges for fixed Δt as $n \to \infty$. While this in principle implies a decay of $\exp[-\Gamma(t)]$ to zero under the PDD, details of the spectral density function (including the nature of the coupling spectrum and the form of spectral cutoff) become essential to characterize different dynamical regimes of interest. In what follows, we illustrate these features by contrasting Ohmic and supra-Ohmic dephasing environments, and by considering *stroboscopic* sampling, $t_n = 2n\Delta t$, in which case explicit analytic expressions for the PDD "filter function" $|y_{2n}(2n\omega\Delta t)|^2$ are available. Specifically, upon combining Eq. (11b) of Ref. [13] with Eq. (12), one recovers the well-known result [1,14,50]

$$\Gamma_{2n}(2n\Delta t) = \int_0^\infty 4\eta(\omega)\sin^2(\omega n\Delta t)\tan^2\left(\frac{\omega\Delta t}{2}\right)d\omega. \quad (27)$$

In general, we expect two dominant contributions to the above integral: the one from small values of ω, where $\eta(\omega)$ is not small, and the one from the region of the resonance, $\omega \approx \omega_{\mathrm{res}}$, where $|y_{2n}(\omega t)|^2$ may be large. First, note that for both Ohmic and supra-Ohmic spectral density, the contributions from the small-ω region saturate to a *finite* value with time. For the Ohmic case, this is true irrespective of the fact that

the free dephasing dynamics does *not* exhibit a similar long-time saturation. This behavior is caused by the control term $\tan^2(\omega \Delta t/2)$, which increases the rate at which the integrand goes to zero as $\omega \to 0$. Second, the contribution from the $\omega \approx \omega_{\text{res}}$ region is more or less relevant depending on the form of the spectral cutoff. Clearly, such resonating contributions do not pose a problem in the limiting situation of an arbitrarily hard spectral cutoff of the form $\Theta(\omega - \omega_c)$ [$\Theta(\,)$ denoting the step function], since, as remarked earlier, $\omega_{\text{res}} > \omega_c$ in a good DD limit. For a smooth (soft) spectral cutoff, the resonating contribution increases with time and will ultimately be responsible for the divergence of $\Gamma_{2n}(2n\Delta t)$ as $n \to \infty$. In fact, $\Delta\Gamma_\infty$ corresponds precisely to such a frequency range. As shown by Eq. (26), we can approximate $\Delta\Gamma_n \approx \Delta\Gamma_\infty$ for $t > t_{\text{sat}}$; since at such long times the contributions to Eq. (27) from small ω have saturated, dephasing is indeed dominated from the region around ω_{res}. Thus, for both Ohmic and supra-Ohmic systems under PDD, the coherence eventually decays to zero for large enough times and sufficiently soft spectral cutoffs.

The above considerations are illustrated in Fig. 4, where we plot exact results calculated from Eq. (27) for a representative
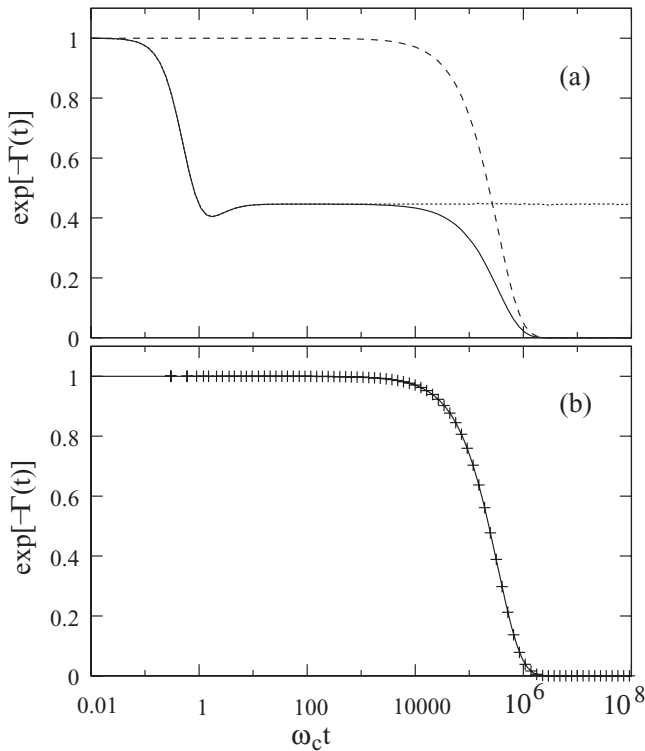

FIG. 4. Dephasing behavior for an Ohmic spectral density with exponential cutoff as in Eq. (28), with $F = 0.5$, $\alpha = 1/2$, $\Delta t = 0.0015$, $\omega_c = 100$, and $T = 100\omega_c$, in units where $\hbar = k_B = 1$. While stroboscopic sampling is implied, continuous interpolating lines are used for clarity of illustration. (a) Full decoherence function, $\exp[-\Gamma(t_n)]$, Eq. (27) (solid line); low-frequency contribution, $\exp[-\Gamma_{\text{sm}\omega}(t)]$, Eq. (29) (dotted line); resonating contribution, $\exp[-\Gamma_{\text{res}}(t)]$, Eq. (30) (dashed line) versus rescaled time $\omega_c t$. (b) Comparison between $\exp[-\Gamma_{\text{res}}(2n\Delta t)]$, Eq. (30) (points), and $\exp(-\Delta\Gamma_\infty t/\Delta t)$ (solid line).

Ohmic spectral density with an exponential cutoff [1]:

$$I_a(\omega) = F\omega \exp\left(-\frac{\omega}{\omega_c}\right). \tag{28}$$

In order to highlight the different contributions to the overall dephasing function, we also explicitly compute and plot the following quantities: (i) (dotted line)

$$\Gamma_{\text{sm}\omega}(2n\Delta t) = \int_0^{\omega_{\text{res}}/2} \eta(\omega)|y_{2n}(\omega 2n\Delta t)|^2 d\omega, \tag{29}$$

which isolates the small-ω contributions, and (ii) (dashed line)

$$\Gamma_{\text{res}}(2n\Delta t) = \int_{\omega_{\text{res}}/2}^{3\omega_{\text{res}}/2} \eta(\omega)|y_{2n}(\omega 2n\Delta t)|^2 d\omega, \tag{30}$$

which isolates the contributions from the $\omega \approx \omega_{\text{res}}$ region. Three distinct regions may be identified: an initial drop in coherence due to the low-frequency modes, until saturation of Eq. (29) occurs at about $t = \tau_c$; a plateau region where the contributions from Eq. (30) are not important enough to cause further decoherence; and a final decay of coherence to zero caused by increasing contributions from the $\omega \approx \omega_{\text{res}}$ region. Figure 4 also compares (bottom panel) the resonating contributions calculated from Eq. (30) with the asymptotic prediction $\exp(-\Delta\Gamma_\infty t/\Delta t)$ (solid line), with $\Delta\Gamma_\infty = 4.507 \times 10^{-7}$. The data confirm that $\Delta\Gamma_\infty$ does indeed arise from the resonating contributions as expected, and that, as long as the low-frequency contributions have saturated, $\Delta\Gamma_\infty$ may be used to accurately describe dephasing under PDD in the long-time limit, that is, $\Delta\Gamma_n \approx \Delta\Gamma_\infty$, for $t > t_{\text{sat}}$.

Additional insight may be gained by examining how the above different regimes (initial decay, plateau, final coherence decay) are affected by the harder or softer spectral cutoff function. In addition to the Ohmic spectral density of Eq. (28), consider the following supra-Ohmic spectral densities:

$$I_b(\omega) = F\omega^3 \exp\left(-\frac{\omega}{\omega_c}\right), \tag{31}$$

$$I_c(\omega) = F\omega^3 \exp\left(-\frac{\omega^2}{\omega_c^2}\right), \tag{32}$$

where, in particular, $I_c(\omega)$ has a Gaussian tail, as in the excitonic qubit case. When $I_b(\omega)$ and $I_c(\omega)$ are compared (see Fig. 5), the harder cutoff owing to the Gaussian tail strongly reduces the value of $\eta(\omega_{\text{res}})$, and hence greatly increases the duration of the plateau regime. In fact, for the set of parameters chosen, our numerics lose the necessary precision well before the third regime sets in for $I_c(\omega)$. The harder cutoff of the Gaussian case also decreases $\Gamma_{\text{sm}\omega}$ and, in turn, decreases the decoherence that occurs before the plateau.

B. Short-time dynamics

In the previous section, we analyzed the dephasing dynamics in the presence of PDD for $t > t_{\text{sat}}$. Here, we focus on $t < t_{\text{sat}}$. The long-time regime is entered when $\Gamma_{n+1} = \Gamma_n + \Delta\Gamma_\infty$, and for this to occur the coherence must oscillate in phase with the DD pulses. However, the natural response of the coherence after the first PDD pulse is instead to oscillate with a period of $2\Delta t$ (twice that of PDD pulses; see Fig. 6). This follows from the fact that the first bit flip occurs an interval Δt after a
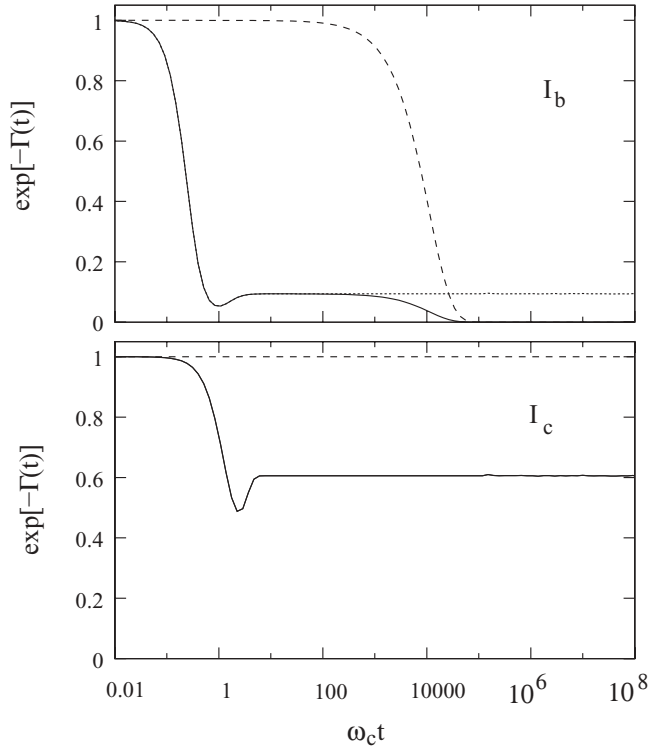
FIG. 5. Dephasing behavior for supra-Ohmic spectral densities with different cutoffs, Eqs. (31) and (32). Notice that now $F = 0.0001$, while all other parameters are as in Fig. 4. $\exp[-\Gamma(t)]$ (solid line), $\exp[-\Gamma_{sm\omega}(t)]$ (dotted line), and $\exp[-\Gamma_{res}(t)]$ (dashed line) as functions of the rescaled time $\omega_c t$ for spectral densities I_b (upper panel) and I_c (lower panel), respectively.

maximum, $\Gamma_0(0)$, and for sufficiently small Δt the dephasing function is roughly symmetrical about the control pulse, so the coherence maximum following the first pulse occurs at $t \approx 2\Delta t$. The PDD sequence quickly drives the coherence into phase with it (see Fig. 6), but the first few *even* bit flips in PDD occur near the coherence maxima, and this worsens the performance of the control sequence. This can be seen by considering Eq. (10) at time $t = t_n + \tilde{t}$, with $0 < \tilde{t} \leqslant \Delta t$. By expanding the first and last terms to first order in $\tilde{t}$, and
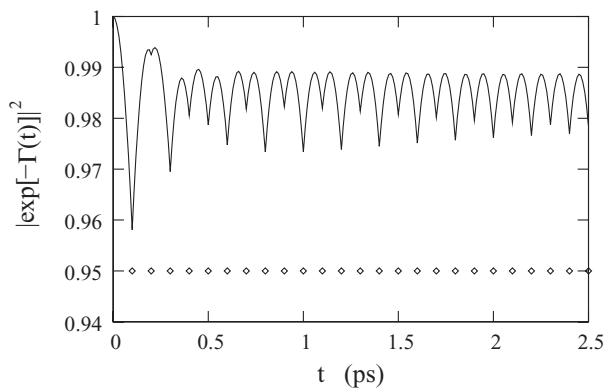

FIG. 6. Short-term dephasing of the exciton qubit under PDD, with $\Delta t = 0.1$ ps. The diamonds indicate the timing of the PDD pulses.

considering that $\Gamma_0(0)$ is a maximum, we can rewrite Eq. (10) as

$$\Gamma_n(t) \approx -\frac{d\Gamma_{n-1}(t_n)}{dt}\tilde{t} + \Gamma_{n-1}(t_n). \qquad (33)$$

The second term in the above equation is a constant; hence there can be a coherence peak after the nth control pulses only if the derivative $d\Gamma_{n-1}(t_n)/dt > 0$, as also pointed out in Ref. [50]. In particular, again using Eq. (10), we can calculate

$$\frac{d\Gamma_n(t_n)}{dt} \approx \frac{\Gamma_n(t_n + \tilde{t}) - \Gamma_n(t_n)}{\tilde{t}} = -\frac{d\Gamma_{n-1}(t_n)}{dt},$$

which shows that the larger the gradient of $\Gamma_{n-1}(t_n)$, the faster the coherence is retrieved immediately following the nth pulse. In particular, if $\Gamma_{n-1}(t)$ is locally flat at the time of the nth pulse, *no coherence gain* can occur after that pulse.

We can see from Fig. 6 that, as PDD drives the coherence oscillations into phase with it, $\Delta\Gamma_n$ has alternating signs for odd and even n [cf. Eqs. (B5) and (B7)]. $\Delta\Gamma_n$ is initially negative for odd n and positive for even n, while its magnitude decreases until a time t_{av} after which $\Delta\Gamma_n$ becomes positive for odd n and negative for even n, before saturating to $\Delta\Gamma_n = \Delta\Gamma_\infty$. We see numerically that t_{av} is independent of Δt, with $t_{av} \approx 0.5$ ps in our case. Furthermore, we can show from Eq. (A1) that, if we consider the times at which the control pulses occur ($\tilde{t} = 0$), then

$$\Delta\Gamma_n^{PDD}(0) = \Delta\Gamma_{n-1}^{PDD}(0) + (-1)^n \Delta t^2 \Gamma_0''(n\Delta t), \qquad (34)$$

where

$$\frac{d^2\Gamma_0(n\Delta t)}{dt^2} = \frac{\Gamma_0[(n-1)\Delta t] - 2\Gamma_0(n\Delta t) + \Gamma_0[(n+1)\Delta t]}{\Delta t^2}.$$

From this expression we can understand the behavior of the dephasing for PDD as the coherence oscillations are driven into phase with the PDD pulses. As n increases, the sign of the last term in Eq. (34) alternates, and its magnitude decreases as $d\Gamma_0(n\Delta t)/dt$ reaches a maximum, before decreasing and tending to zero [recall the behavior of $\Gamma_0(t)$ in Fig. 1]. Thus, we can now rigorously define t_{av} by the condition $d^2\Gamma_0(t_{av})/dt^2 = 0$, that is, when the gradient of $\Gamma_0(t)$ is maximum.

C. Practical considerations

Even if the qubit coherence eventually decays to zero under PDD in our excitonic system, for practical purposes we need to suppress the dephasing only for the qubit lifetime T_1. From the above discussion, we can estimate more precisely how short Δt must be, in order for this to happen. For $t = n\Delta t + \Delta t/2 > t_{sat}$, we can approximate the off-diagonal density matrix element at the maxima of coherence (where a measurement would be made) as

$$\rho_{01}[(n+1/2)\Delta t] \approx \rho_{01}(0)e^{-\Gamma_{n_{sat}}[(n_{sat}+1/2)\Delta t] - (n-n_{sat})\Delta\Gamma_\infty}. \qquad (35)$$

Considering the long-time limit, if Δt is sufficiently small and $n \gg n_{sat}$, we may neglect the coherence that is lost while $t < t_{sat}$, and further approximate the dephasing as

$$\rho_{01}[(n+1/2)\Delta t] \approx \rho_{01}(0)e^{-n\Delta\Gamma_\infty} \approx \rho_{01}(0)e^{-(\Delta\Gamma_\infty/\Delta t)t}. \qquad (36)$$
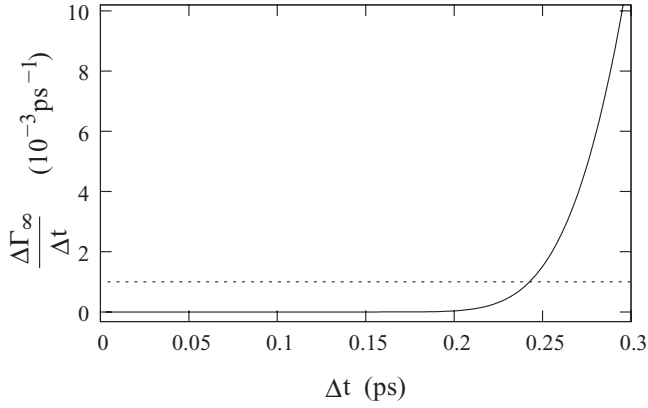
FIG. 7. Effective long-time coherence decay rate, $1/T_2^{\text{eff}} = \Delta\Gamma_\infty/\Delta t$, Eq. (37), as a function of Δt. The dashed line is the qubit inverse lifetime, $1/T_1 = 1$ ns^{-1}.

Thus, in the long-time limit, we effectively have $1/T_2^{\text{eff}} = \Delta\Gamma_\infty/\Delta t$. A sufficient condition for the dephasing to be suppressed for the entire qubit lifetime is then

$$T_2^{\text{eff}} = \frac{\Delta t}{\Delta\Gamma_\infty} \gtrsim T_1. \tag{37}$$

Figure 7 shows $\Delta\Gamma_\infty/\Delta t$ as a function of Δt for the exciton qubit under consideration, for which $1/T_1 = 1$ ns^{-1}. It can be seen that, for $\Delta t \lesssim 0.2$ ps, PDD effectively suppresses dephasing for the entire lifetime. This is in excellent agreement with our previous results in Ref. [38], where we found numerically that $\Delta t = 0.2$ ps leads to efficient PDD, but, in comparison, $\Delta t = 0.3$ ps could suppress the dephasing for only relatively short times.

IV. COMPARISON OF PDD WITH NONUNIFORM DD SCHEMES

Having characterized the performance of the simplest DD scheme, where the control involves a single time scale Δt, we proceed to examine some of the high-level protocols mentioned in the introduction, which involve *nonuniform pulse delays* to a lesser or greater extent. While CPDD is both, historically, the most established approach and, ultimately, one of the most effective, we defer its discussion until after the analysis of CDD and UDD, since it turns out that for the supra-Ohmic system at hand CPDD naturally suggests the optimization strategy that will be introduced in Sec. V.

A. Concatenated decoupling

Instead of repeating the basic control cycle given in Eq. (21), CDD recursively concatenates it within itself. Let S_ℓ denote the sequence corresponding to the ℓth level of concatenation, as given in Table I. For a qubit undergoing arbitrary decoherence, CDD with a "universal decoupling" cycle given, for instance, by $\Delta t X \Delta t Z \Delta t X \Delta t Z$, has been shown [9] to significantly outperform PDD in the limit $\Delta t \to 0$. However, for purely dephasing systems for which Δt has a *finite* lower limit, and for *single-axis* protocols constructed out of the basic cycle in

TABLE I. Concatenated pulse sequences for a purely dephasing single-qubit interaction. Time ordering is from right to left.

Sequence	Pulse timing
S_0	Free(Δt)
S_1	$X \Delta t X \Delta t$
S_2	$X[X \Delta t X \Delta t]X[X \Delta t X \Delta t] = \Delta t X \Delta t \Delta t X \Delta t$
S_3	$X[\Delta t X \Delta t \Delta t X \Delta t]X[\Delta t X \Delta t \Delta t X \Delta t]$
$\vdots$	$\vdots$
S_ℓ	$X S_{\ell-1} X S_{\ell-1}$

Eq. (21), the advantages of CDD are largely lost, and PDD may be more efficient [48]. While different ways for comparing different DD protocols can be considered [9,26,28], we shall focus here on comparing the efficiency of PDD and CDD at ensuring dephasing-protected storage of the exciton qubit for a *fixed* time T_{storage}. In particular, for our calculations we choose $T_{\text{storage}} = 10$ ps. This time is appropriate given the typical gating time for exciton-based QIP, which is of the order of 1 ps [33].

1. Single CDD cycle

Given T_{storage} and the presence of a physical constraint on Δt, a first way to exploit CDD is to identify a minimum concatenation level ℓ^* for which the length of the corresponding sequence, $T_{\ell^*} = 2^{\ell^*}\Delta t$, exceeds T_{storage}. For a given Δt, increase in ℓ beyond this point would not modify the results because the pulse timings over T_{storage} would be unchanged. (see Table I). Figure 8 compares CDD and PDD for storage of an exciton qubit for different Δt. As expected from the general analysis of Ref. [9], the efficiency of CDD increases with decreasing Δt. However, in the range of values under exploration and with readout effected at the maxima of the coherence curve, CDD is found to be more efficient than PDD only if $\Delta t \lesssim 0.036$ ps. This time scale is substantially smaller than is physically allowed in our system.

We can understand the possible advantage of CDD by comparing it with the long- and shorttime behavior of PDD (Secs. III A and III B, respectively). Equation (35) shows that the long-time performance of the protocol depends on $\Delta\Gamma_\infty$, and $\Gamma_{n_{\text{sat}}}[(n_{\text{sat}} + 1/2)\Delta t]$. For very small Δt (hence small $\Delta\Gamma_\infty$), PDD is not the most efficient scheme because it leads to a value of $\Gamma_{n_{\text{sat}}}[(n_{\text{sat}} + 1/2)\Delta t]$, which may be greater than for other pulse sequences, owing to the initially out-of-phase pulses. In the regime where CDD outperforms PDD (very small Δt), the contributions to dephasing from around $\omega = \omega_{\text{res}}$ (see Sec. III A) are negligible for both sequences over T_{storage}, since for $t > t_{\text{sat}}$ both sequences preserve the maxima of coherence very close to the value $\exp[-\Gamma(t_{\text{sat}}^{\text{max}})]$ corresponding to the time $t_{\text{sat}}^{\text{max}}$ of the first maximum that follows t_{sat}. The advantage of CDD (if any) comes from the different behavior of the dephasing over the first few control pulses, that is, up to $t = t_{\text{sat}}$. The timing of the pulses in the CDD sequence is similar to those of PDD, but with fewer pulses at the instants where the even pulses occur in PDD. These "missing" pulses are those that would occur near the maxima of coherence in the initial stages of the sequence (see
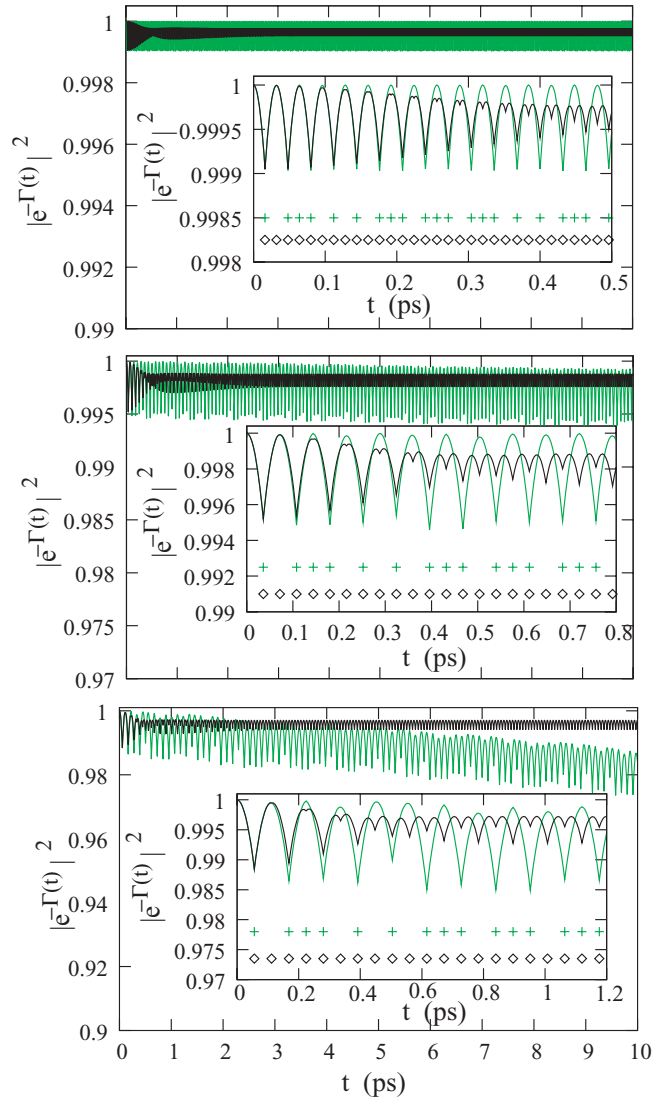
FIG. 8. (Color online) $|\exp[-\Gamma(t)]|^2$ for PDD (black line) compared with CDD (light line) for $\Delta t = 0.016$ ps ($\ell^* = 10$, top), $\Delta t = 0.036$ ps ($\ell^* = 9$, middle), and $\Delta t = 0.055$ ps ($\ell^* = 8$, bottom). Insets: Closeups of the same evolutions at short times; the pulse timings are indicated as well, with crosses (CDD) and diamonds (PDD).

insets of Fig. 8), that is, the ones responsible for decreasing the coherence maxima while $t < t_{\text{sat}}$ in PDD (Sec. III B). These missing pulses allow the dephasing to maintain its natural response frequency after the first bit flip, and no loss of dephasing is needed to change the rate of the oscillations of coherence. Therefore, $\Gamma^{\text{CDD}}(t_{\text{sat}}^{\max}) < \Gamma^{\text{PDD}}(t_{\text{sat}}^{\max})$, and, for $t < T_{\text{storage}}$, $\Gamma(t) \approx \Gamma(t_{\text{sat}}^{\max})$ for both PDD and CDD in the limit of sufficiently small Δt.

While this explains why CDD may outperform PDD, as soon as Δt is long enough such that $\Delta\Gamma_\infty$ is significant compared to T_{storage}, PDD becomes the more efficient sequence. The period of the coherence oscillations for CDD is twice that for the PDD sequence corresponding to the same Δt (see insets in Fig. 8), resulting in faster dephasing at long evolution times t for CDD.

2. Periodic repetition of CDD cycles

A different use of CDD consists in truncating concatenation at a fixed level and periodically repeating the resulting supercycle, constructed from Table I. For instance, truncation at $\ell = 2$ results in our purely dephasing case in a cycle of length $4\Delta t$, which is identical in structure to a CP cycle (see Sec. IV C), and whose periodic repetition we term PCDD$_2$. For a single qubit undergoing arbitrary decoherence, the corresponding PCDD$_2$ protocol (constructed from a 16-pulse base cycle) has been shown to be the best performer in suppressing the effects of a quantum spin bath [26,49,51].

Figure 9 shows a comparison of PDD and PCDD$_\ell$ protocols for $\ell = 2,3$, for the shortest pulse separation compatible with the exciton qubit constraint, $\Delta t = 0.1$ ps. One can infer that, for the Δt and T_{storage} values considered, PCDD$_\ell$ performs better (that is, displays higher coherence maxima) than PDD for $\ell = 2$, but worse for $\ell = 3$. The difference between PCDD$_2$ and PCDD$_3$ may be understood as a consequence of the fact that, in terms of a Magnus expansion [6], concatenated cycles with even ℓ are time symmetric, and thus cancel the interaction with the phonon bath up to (at least) the second order. Over the time period shown, PCDD$_2$ also outperforms standard PDD (see Fig. 9, upper panel). However, the coherence oscillations for PCDD$_2$ occur over a period of $2\Delta t$ since, after the initial pulse, the sequence is equivalent to PDD with a base time interval of $2\Delta t$. Therefore, we expect PDD to be more efficient for long storage times, as PCDD$_2$ will yield a larger $\Delta\Gamma_\infty$ than a PDD sequence characterized by Δt and hence worse asymptotic performance.
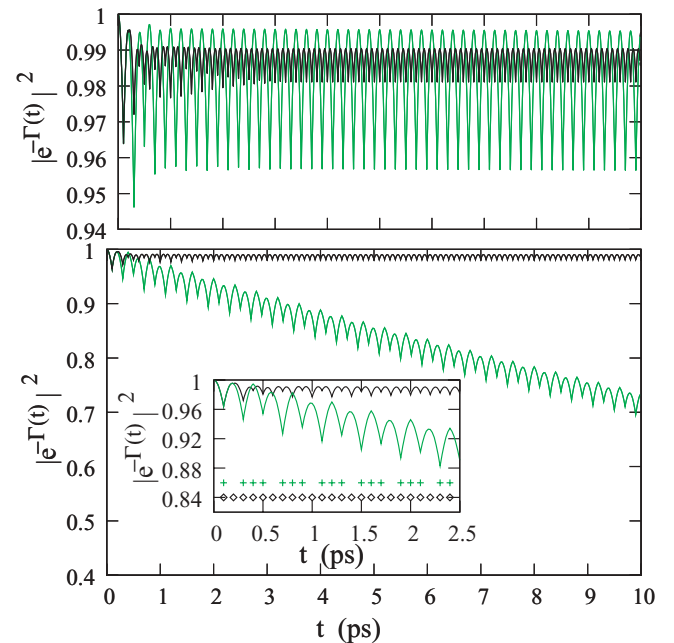

FIG. 9. (Color online) Comparison of PDD (dark line) and PCDD (light line) protocols with $\Delta t = 0.1$ ps. Top: Second-level concatenated cycle, PCDD$_2$. Bottom: Third-level concatenated cycle, PCDD$_3$. Inset: Enlargement of the initial part of the time window with timings of the pulse sequences explicitly indicated (diamonds for PDD and crosses for PCDD$_3$).

B. Uhrig decoupling

We now assess the limitations of the optimal sequence proposed by Uhrig [13] when significant restrictions on Δt are in place. In UDD, consecutive pulses are spaced according to

$$\delta_j = \sin^2\left(\frac{\pi j}{2n+2}\right), \tag{38}$$

which implies, in particular, closely spaced pulses at the beginning and the end of the evolution period. Such a control sequence strongly suppresses the dephasing for a storage time of the order of [13]

$$t_{\text{UDD}} \approx (n+1)\frac{\tau_c}{2\pi}, \tag{39}$$

where τ_c denotes, as before (Sec. III), the relevant bath correlation time. As mentioned, with $\hbar\omega_c \approx 2$ meV, this corresponds to $\tau_c \approx 2.06$ ps. Beyond t_{UDD}, the efficiency of UDD falls rapidly. From Eq. (39), we find that for UDD to efficiently protect the exciton qubit over $T_{\text{storage}} \approx 10$ ps, n must be on the order of 100. Figure 10 shows the resulting UDD performance as n is decreased. It can be seen that as $n \lesssim 100$ the advantage of UDD is rapidly lost.

For our QD system, however, the main physical limitation is on the time delay between pulses. The shortest interval between control pulses in UDD, $\Delta t_{\text{min}}^{\text{UDD}}$, is before the first pulse and after the last pulse. From Eq. (38) we see that such a sequence with $n = 100$ pulses over a period of $T_{\text{storage}} = 10$ ps corresponds to $\Delta t_{\text{min}}^{\text{UDD}} = 2.4 \times 10^{-3}$ ps, which is roughly *two orders of magnitude* less than that allowed by the physical constraints for the exciton qubit in question. Even for a sequence consisting of $n = 40$ pulses only [for which the efficiency is already poor as shown in Fig. 10, curve (c)], $\Delta t_{\text{min}}^{\text{UDD}} = 1.5 \times 10^{-2}$ ps, which is still an order of magnitude shorter than allowed.

To respect the physical constraints, one may estimate that allowed UDD sequences should have a number of pulses $n \lesssim 14$ within the intended $T_{\text{storage}} = 10$ ps. Such a sequence corresponds to curve (e) in Fig. 10. It is then clear that any UDD sequence compatible with our physical constraints is outperformed by the best allowed PDD sequence that would preserve a coherence close to 1 for the same time window
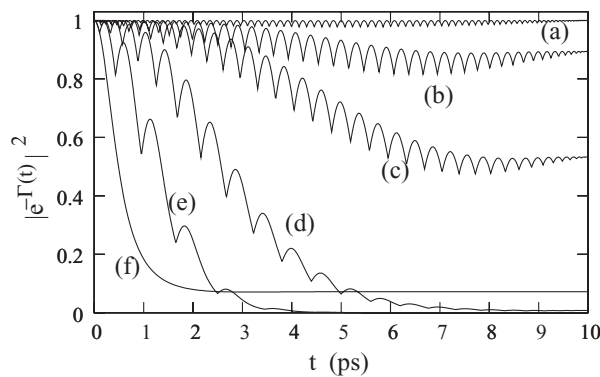

FIG. 10. $|\exp[-\Gamma(t)]|^2$ for the exciton qubit in the presence of UDD with (a) 100, (b) 50, (c) 40, (d) 25, and (e) 14 pulses corresponding to the best allowed sequence for the case of the exciton qubit. For comparison, (f) shows the free evolution.

(see Fig. 2). Figure 10 also shows that any constrained UDD sequence performing like curve (d) or worse would increase the dephasing compared with the free evolution, that is, would result in decoherence acceleration. The reason for the shortfalls of UDD in our setting stems from the large spread of the control intervals $(t_i - t_{i-1})$. If we impose a lower bound on the minimum time interval, other intervals must take up a considerable proportion of the total evolution time. This places a relatively large restriction on how many pulses may be used within a given storage period, and eventually results in large amounts of dephasing during the long time delays in which no pulses occur. Related conclusions, supporting the limitations of UDD sequences in the presence of a finite minimum pulse interval, have been independently reported in Ref. [53] in the context of rigorous perturbative error bounds.

C. Carr-Purcell decoupling

We now focus on analyzing more closely CPDD, which results from the periodic repetition of a CP cycle of the form [7]

$$\Delta t^{\text{CP}} X 2\Delta t^{\text{CP}} X \Delta t^{\text{CP}}. \tag{40}$$

This also corresponds, as noted, to PCDD$_2$ with $\Delta t^{\text{CP}} = \Delta t$ (cf. Table I). Specifically, we are interested in comparing a PDD sequence with a CPDD having the *same cycle time* $T_c = 2\Delta t$ and thus $\Delta t^{\text{CP}} = \Delta t/2$: although the corresponding pulse time interval may not be allowed by the physical constraints we are considering, this study will pave the way to the analysis developed in the next section.

Basically, CPDD may be viewed as a PDD protocol where pulses are uniformly spaced by $2\Delta t^{\text{CP}}$, except that the sequence is displaced forward by $t_1 = \Delta t/2$, the time at which the first pulse is applied. As a consequence of the symmetry of the control propagator in Eq. (40) with respect to the cycle midpoint, it is well known [5] that CPDD is a second-order protocol as compared to standard (asymmetric) PDD, with leading corrections of order T_c^3. Using the exact representation established in Eq. (11), we will now assess the extent to which CPDD improves over PDD for a purely dephasing system, and gain insight into asymptotic properties.

We begin by determining the dephasing halfway between consecutive control pulses for the case of PDD. Using Eq. (11), we find

$$\Gamma_n^{\text{PDD}}\left[t = \left(n+\frac{1}{2}\right)\Delta t\right]$$

$$= 2\sum_{m=1}^{n}(-1)^{m+1}\Gamma_0(m\Delta t)$$

$$+ 4\sum_{m=2}^{n}\sum_{j<m}\Gamma_0[(m-j)\Delta t](-1)^{m-1+j}$$

$$+ 2\sum_{m=1}^{n}(-1)^{m+n}\Gamma_0\left[\left(n+\frac{1}{2}-m\right)\Delta t\right]$$

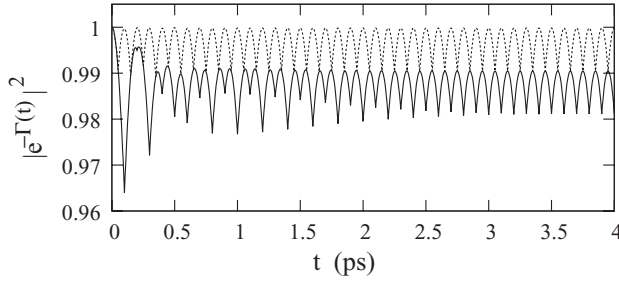$$+ (-1)^n\Gamma_0\left[\left(n+\frac{1}{2}\right)\Delta t\right], \tag{41}$$

FIG. 11. Comparison of CPDD (dotted line) with $\Delta t^{CP} = 0.05$ ps and PDD (solid line) with $\Delta t = 0.1$ ps for the exciton system.

which we may rewrite as

$$
\Gamma_n^{PDD}\left[\left(n + \frac{1}{2}\right)\Delta t\right]
$$
$$
= 2\sum_{m=1}^{n}(-1)^{m+1}\Gamma_0(m\Delta t)
$$
$$
+ 4\sum_{m=2}^{n}\sum_{j<m}\Gamma_0[(m-j)\Delta t](-1)^{m-1+j}
$$
$$
+ 2\sum_{k=1}^{n}(-1)^{k+1}\Gamma_0\left[\left(k - \frac{1}{2}\right)\Delta t\right]
$$
$$
+ (-1)^n\Gamma_0\left[\left(n + \frac{1}{2}\right)\Delta t\right], \tag{42}
$$

where $k = n - m + 1$. Similarly, by using Eq. (11), we may also determine the dephasing for CPDD with $\Delta t^{CP} = \Delta t/2$ and $t_i = (i - 1/2)\Delta t$, that is,

$$
\Gamma_n^{PDD}[(n + 1/2)\Delta t] = \Gamma_n^{CPDD}[(n + 1/2)\Delta t]. \tag{43}
$$

This *exact* result is illustrated in Fig. 11, where we plot the dephasing behavior under PDD and CPDD for the exciton qubit with $\Delta t = 0.1$ ps. As predicted by Eq. (43), the coherence in the presence of each sequence is equal at times $t = (n + 1/2)\Delta t$. Interestingly, for $t > t_{sat}$, $\Gamma_n^{PDD}[(n + 1/2)\Delta t]$ are local maxima of coherence whereas $\Gamma_n^{CPDD}[(n + 1/2)\Delta t]$ are local minima, proving CPDD to be much more efficient than PDD provided that the time of the first pulse is allowed to be $t_1 = 0.05$ ps.

V. TOWARDS OPTIMIZED SEQUENCES IN THE PRESENCE OF PULSE TIMING CONSTRAINTS

Building on the understanding gained from the comparison between different protocols in Sec. IV, we now specifically aim to optimize DD performance for a bosonic dephasing environment when pulses are subject to a minimum pulse-delay constraint. The basic observation is to note that if, after an initial arbitrary pulse sequence, PDD is turned on at a time t_{PDD}, then for $t > t_{PDD} + t_{sat}$ we have $\Gamma_{n+1}(t + \Delta t) - \Gamma_n(t) = \Delta\Gamma_\infty$ [recall Eq. (26)]. This naturally suggests an *interpolated DD* approach, where an initial sequence is chosen to minimize $\Gamma(t_{sat}^{max})$, while transforming the oscillations of coherence into phase with a PDD sequence to be turned on immediately afterwards. Interestingly, a similar philosophy has been invoked to optimally merge deterministic and randomized DD methods

to enhance performance over the entire storage time [54]. In our case, CPDD is indeed the simplest example of this interpolation: as already noted, CPDD can be thought of as a PDD sequence applied at $t_{PDD} = \Delta t/2 + \Delta t$, following a preparatory sequence consisting of a single pulse at $t = \Delta t/2$.

Unfortunately, standard CPDD is not allowed in our system because of the physical constraint: the time interval between pulses in the initial sequence is smaller than the minimum allowed Δt that characterizes the subsequent PDD sequence. Simply using a CPDD sequence which does not break the time constraint is clearly not optimal. If the smallest allowed pulse interval is Δt_{min}, then the best CPDD sequence consists of periodic repetitions of a CPDD cycle with $\Delta t^{CP} = \Delta t_{min}$, and the most efficient allowed PDD sequence is repetitions of $X\Delta t_{min}X\Delta t_{min}$. Since CPDD cancels the terms in the Magnus expansion up to to the second order, over the first few repetitions it performs much better than PDD, which cancels them up only to the first order. However, for longer times the effects due to the higher-order Magnus corrections accumulate, and they turn out to do so more favorably for PDD. This manifests itself in a smaller $\Delta\Gamma_\infty$ for PDD than for the best allowed CPDD protocol. As shown by Eqs. (B3) and (B6), the coherence oscillations are independent of the timing of any pulses applied before $t - t_{sat}$. Therefore, CPDD can be treated as a PDD sequence with $\Delta t = 2\Delta t^{CP}$ for $t > t_{sat}$. This justifies the definition of a $\Delta\Gamma_\infty$ for a CPDD sequence.

Physically, what is needed is a different initial sequence that efficiently "engineers" the transition of the coherence oscillations—from the natural response frequency determined by the first bit flip to the frequency of the following PPD sequence. To accomplish this, we propose to use *CP cycles with varying* Δt^{CP}. That is, we define such an interpolated sequence by letting the ith cycle be characterized by a pulse delay Δt_i^{CP}, and begin immediately after the previous cycle at $t_i = t_{i-1} + 4\Delta t_{i-1}^{CP}$. The analysis of the resulting averaging properties may be carried out by adapting the derivation of Ref. [9] to the pure dephasing bosonic setting of Eq. (1). While the details of the calculations are included in Appendix C, the result is that, as with the standard CP cycle, the proposed DD sequence still cancels the terms in the Magnus expansion up to the second order. Therefore, the interpolated scheme not only performs well for small t, but also quickly results in pulses uniformly separated by Δt_{min}, resulting in a small $\Delta\Gamma_\infty$ and hence high performance for long storage times.

The simplest way to generate a good interpolated DD sequence is to apply a CP cycle with $\Delta t^{CP} = \Delta t_{min}$, followed by periodic repetitions of one with $\Delta t^{CP} = \Delta t_{min}/2$. The sequence is then given by

$$
\begin{aligned}
t_1 &= \Delta t_{min}, \\
t_2 &= 3\Delta t_{min}, \\
t_3 &= 3\Delta t_{min} + \tfrac{3}{2}\Delta t_{min}, \\
t_i &= t_{i-1} + \Delta t_{min}, \quad i > 3.
\end{aligned} \tag{44}
$$

We compare this sequence with standard PDD with $\Delta t = \Delta t_{min}$ in Fig. 12, upper panel. One clearly sees that the sequence in Eq. (44) is more efficient.

By construction, the first two CP cycles in the above sequence play the role of modifying the frequency of the
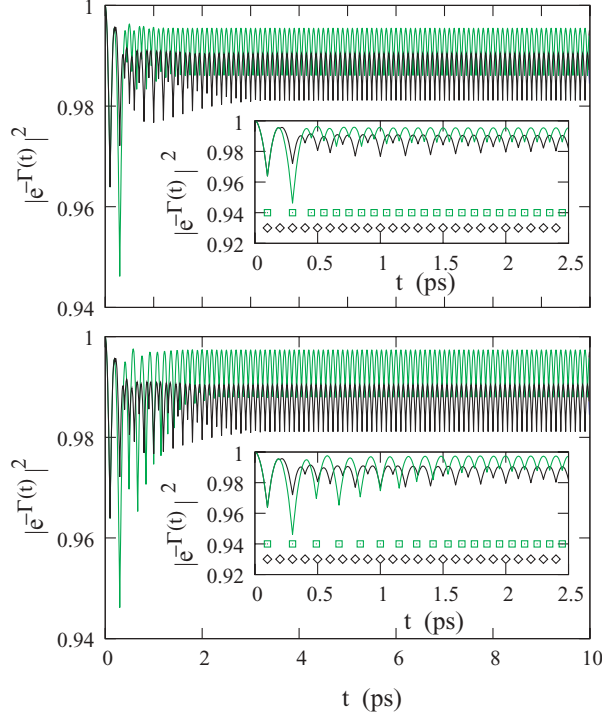
FIG. 12. (Color online) Comparison of PDD (dark line) with interpolated DD sequences of varying CP cycles (light line), for $\Delta t_{\min} = 0.1$ ps. Top: Sequence given by Eq. (44). Bottom: Sequence given by Eq. (45), with $\Delta_2 = 0.01$ ps. Inset: Enlargement of the initial part of the time window with timings of the pulse sequences explicitly indicated (diamonds for PDD and squares for the modified sequences).

dephasing oscillations in such a way that they are brought in phase with the following repeated cycles. We can perform this process more smoothly by gradually reducing Δt^{CP} from $\Delta t_{\min}$ to $\Delta t_{\min}/2$ over more than a control cycle. Although for very small $\Delta t_{\min}$ the two cases would be equivalent, for systems such as the exciton qubit, where the time restrictions are relatively severe, the smoother transition sequence may decouple the qubit more efficiently. Such a modified sequence may be implemented by applying CP cycles with decreasing Δt^{CP}, that is,

$$\Delta t_i^{\mathrm{CP}} = \begin{cases} \Delta t_{\min}, & i = 1, \\ \Delta t_{\min} - (i-1)\Delta_2, & 1 < i \leqslant i_{\mathrm{PDD}}, \\ \Delta t_{\min}/2, & i > i_{\mathrm{PDD}}, \end{cases} \quad (45)$$

where $i_{\mathrm{PDD}} = \Delta t_{\min}/(2\Delta_2)$ and Δ_2 is an arbitrary time defined such that i_{PDD} is an integer. The greater i_{PDD}, the longer the time over which the the decreasing length cycles are applied. Alternatively, we may describe the above sequence in terms of the pulse times:

$$t_i = \Delta t_{\min} + (i-1)2\Delta t_{\min} - \frac{(i-1)(i-2)}{2}\Delta_2, \quad i < \frac{\Delta t_{\min}}{\Delta_2} - 2, \quad (46)$$

$$t_i = t_{i-1} + \Delta t_{\min}, \quad i \geqslant \frac{\Delta t_{\min}}{\Delta_2} - 2.$$

The above modified sequence is compared to PDD with $\Delta t = \Delta t_{\min}$ in Fig. 12, lower panel. As before, we see that DD
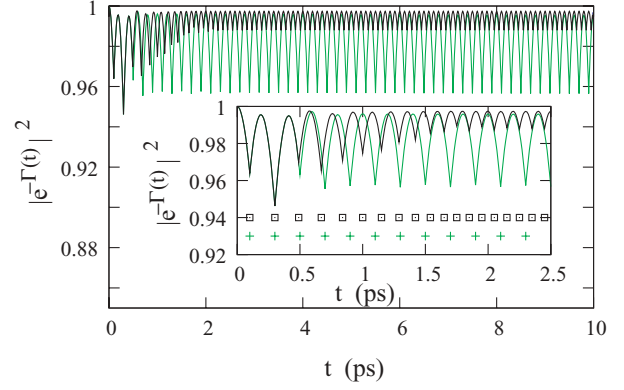

FIG. 13. (Color online) Comparison of the best allowed CPDD sequence (light line) with a sequence of CP cycles of decreasing length (dark line) as described in Eq. (45) with $\Delta_2 = 0.01$ ps and for $\Delta t_{\min} = 0.1$ ps. Inset: Enlargement of the initial part of the time window with timings of the pulse sequences explicitly indicated (squares for the modified sequence and crosses for CPDD, respectively).

with varying CP cycles outperforms PDD. Furthermore, it can be seen that there is an improvement over the more abrupt sequence described by Eq. (44).

In Sec. IV A 2, we showed that a constrained CPDD sequence could outperform PDD over time scales of the order of 10 ps (see top panel of Fig. 9 for PCDD$_2$) even though, for longer times, the smaller $\Delta\Gamma_\infty$ for PDD would eventually make it more efficient than CPDD. In Fig. 13, we further compare CPDD with the interpolated sequence given in Eq. (45). The latter is found to be slightly more efficient than the best allowed CPDD sequence over short time scales. Furthermore, because of the smaller $\Delta\Gamma_\infty$, as time progresses it will also outperform CPDD asymptotically. A main advantage of the sequence given in Eq. (45), however, is that it not only leads to higher maxima than CPDD, but also, after the first few pulses, to a *much smaller coherence oscillation amplitude*. This reflects the fact that the oscillation period has been tuned to the minimum allowed time interval $\Delta t_{\min}$. In this respect, the performance of the sequence in Eq. (45) is more robust against the precise readout times, or, equivalently, a readout offset error relative to the coherence maxima would not significantly affect the coherence recovered using this sequence.

VI. CONCLUSION AND OUTLOOK

We have investigated the ability of DD to inhibit decoherence of a single qubit coupled to a purely dephasing environment, with focus on comparing the performance of low-level periodic DD schemes based on uniform pulse separations to higher-level nonuniform DD schemes.

Our starting point is provided by an exact representation of the controlled decoherence dynamics in terms of the uncontrolled (free) evolution, Eq. (11). While the latter is available provided that control pulses may be regarded as effectively instantaneous, dephasing processes arising from either a bosonic quantum environment or a classical fluctuating environment are encompassed with minor modifications. For bosonic environments, in particular, we have illustrated the

usefulness of our exact representation by obtaining rigorous results for the asymptotic coherence dynamics in the presence of periodic DD. Building on this analysis, we have shown that a main weakness of PDD is due to the oscillation of coherence following the first bit flip being out of phase with the rest of the sequence. This has naturally suggested the application of a suitably engineered preparatory sequence as a strategy to enhance DD efficiency, by bringing the coherence oscillations into phase with a subsequent PDD sequence. The resulting interpolated DD protocols are found to be especially efficient for physical systems where the mimimum time interval between control pulses is strongly constrained. For such systems, DD protocols like concatenated or Uhrig DD, which are designed to achieve peak performance when the asymptotic regime of arbitrarily small pulse separations is fully accessible, tend to largely lose their advantages.

For the excitonic supra-Ohmic dephasing environment of interest, in particular, we have shown how a sequence of Carr-Purcell cycles with suitably chosen (analytically generated) time delays provides a very efficient DD protocol for realistic QD parameters and qubit storage times. Our process of constructing a DD sequence under which the coherence oscillates asymptotically with the minimum period allowed by the physical contraints offers, as a by-product, the advantage of a *significantly smaller coherence oscillation amplitude*, relative to constrained PCDD or UDD sequences. This makes the proposed interpolated sequence more *robust* against readout.

While our analytically designed interpolated DD protocol might be compelling in its simplicity, identification of DD schemes that are guaranteed to yield optimal performance subject to nontrivial timing constraints appears as an interesting control-theoretic problem for further investigation. reconsideration of the local numerical optimization approach recently proposed in Ref. [19] in a *constrained minimization* perspective might offer a concrete starting point in this respect. Likewise, the investigation of dynamical error-control schemes based on bounded-strength Eulerian DD [55], along with the recently proposed extension to decoherence-protected quantum gates [56,57], might prove especially fruitful for exciton qubits, in view of the reduced control overheads associated with purely dephasing environments. Lastly, an interesting general question is under which circumstances (or limiting conditions) a representation of the controlled coherence dynamics in terms of the uncontrolled one might be established for an *arbitrary* purely dephasing error model. This would enable one, for instance, to gain additional insight into the controlled dynamics of systems exposed to non-Gaussian classical phase noise [28] or dephasing caused by a quantum spin bath [58].

APPENDIX A: DERIVATION OF $\Delta\Gamma_\infty$

For PDD, $t_n = n\Delta t$; using this expression and recasting the sums in Eq. (23) in terms of $k = n - j$, we can write

$$\Delta\Gamma_n^{\text{PDD}} = (-1)^n\Gamma_0[(n+1)\Delta t] - 3\Gamma_0(n\Delta t)(-1)^n$$
$$- 4\sum_{k=1}^{n-1}\Gamma_0(k\Delta t)(-1)^k. \qquad (A1)$$

Using Eq. (6) for $n = 0$ and extending the sum to include $k = 0$, Eq. (A1) becomes

$$\Delta\Gamma_n^{\text{PDD}} = -4\int_0^\infty \eta(\omega)d\omega + (-1)^n\int_0^\infty 6\eta(\omega)\cos(\omega n\Delta t)d\omega$$
$$- (-1)^n\int_0^\infty 2\eta(\omega)\cos[\omega(n+1)\Delta t]d\omega$$
$$+ 8\int_0^\infty \eta(\omega)\sum_{k=0}^{n-1}\cos(\omega k\Delta t)(-1)^k d\omega. \qquad (A2)$$

By using the relationship

$$\sum_{k=1}^{n}(-1)^k\cos(kx) = -\frac{1}{2} + \frac{(-1)^n\cos\left(\frac{2n+1}{2}x\right)}{2\cos\left(\frac{x}{2}\right)}, \qquad (A3)$$

we can rewrite the above equation as

$$\Delta\Gamma_n^{\text{PDD}} = 2\int_0^\infty \eta(\omega)\left\{(-1)^{n+1}\cos[(n+1)\omega n\Delta t]\right.$$
$$+ (-1)^{n+1}\cos(n\omega n\Delta t)$$
$$\left.+ 2\frac{(-1)^n\cos\left(\frac{2n+1}{2}\Delta t\omega\right)}{\cos\left(\frac{\Delta t\omega}{2}\right)}\right\}d\omega$$
$$= 4\int_0^\infty \eta(\omega)\left\{(-1)^{n+1}\cos\left(\frac{2n+1}{2}\Delta t\omega\right)\right.$$
$$\left.\times\cos\left(\frac{\Delta t\omega}{2}\right) + \frac{(-1)^n\cos\left(\frac{2n+1}{2}\Delta t\omega\right)}{\cos\left(\frac{\Delta t\omega}{2}\right)}\right\}d\omega. \qquad (A4)$$

This finally can be rearranged as

$$\Delta\Gamma_n^{\text{PDD}} = 4\int_0^\infty \eta(\omega)\sin^2\left(\frac{\omega\Delta t}{2}\right)$$
$$\times \frac{(-1)^n\cos\left[\omega\left(n+\frac{1}{2}\right)\Delta t\right]}{\cos\left(\frac{\omega\Delta t}{2}\right)}d\omega. \qquad (A5)$$

We now take the limit of $n \to \infty$, and note that

$$\lim_{n\to\infty}\frac{(-1)^n\cos\left[\omega\left(n+\frac{1}{2}\right)\Delta t\right]}{\cos\left(\frac{\omega\Delta t}{2}\right)}\frac{1}{2\pi}$$
$$= \frac{1}{\Delta t}\sum_{l=0}^\infty \delta[\omega - (\omega_{\text{res}} + 2l\omega_{\text{res}})]. \qquad (A6)$$

If we assume that $\eta(\omega_{\text{res}}) \gg \eta(\omega_{\text{res}} + 2l\omega_{\text{res}})$ for $l > 0$, which is true for sufficiently small Δt (that is, $\omega_{\text{res}} \gg \omega_c$), we can

neglect contributions from $l > 0$ and define

$$\Delta\Gamma_\infty = \lim_{n\to\infty} \Delta\Gamma_n^{\text{PDD}} \tag{A7}$$

$$= \int_0^\infty 8\delta(\omega - \omega_{\text{res}})\eta(\omega)\omega_{\text{res}}\sin^2\left(\frac{\omega\Delta t}{2}\right)d\omega$$

$$= 8\eta(\omega_{\text{res}})\omega_{\text{res}}.$$

APPENDIX B: LONG-TIME LIMIT OF $\Delta\Gamma_n^{\text{PDD}}(\tilde{t})$

By using Eq. (11) and straightforward manipulations, we can separate $\Delta\Gamma_n^{\text{PDD}}(\tilde{t})$ from Eq. (25) into two parts,

$$\Delta\Gamma_n^{\text{PDD}}(\tilde{t}) = \Delta\Gamma_n^{TI} + \Delta\Gamma_n^{\text{TD}}(\tilde{t}), \tag{B1}$$

with

$$\Delta\Gamma_n^{\text{TD}}(\tilde{t}) = (-1)^n[\Gamma_0(t_n + \tilde{t}) - \Gamma_0(t_{n+1} + \tilde{t})], \tag{B2}$$

and the second term

$$\Delta\Gamma_n^{\text{TI}} = 2(-1)^n \left(\Gamma_0(t_{n+1}) + 2\sum_{j=1}^n (-1)^j\Gamma_0(t_{n+1} - t_j) \right), \tag{B3}$$

independent of $\tilde{t}$. By using

$$\Gamma_0(t) = 2\int_0^\infty \eta(\omega)[1 - \cos(\omega t)]d\omega, \tag{B4}$$

we can rewrite $\Delta\Gamma_n^{\text{TD}}(\tilde{t})$ as

$$\Delta\Gamma_n^{\text{TD}}(\tilde{t}) = -4(-1)^n \int_0^\infty \eta(\omega)\sin\left(\frac{\Delta t\omega}{2}\right)$$

$$\times \sin\left\{\left[\left(n + \frac{1}{2}\right)\Delta t + \tilde{t}\right]\omega\right\}d\omega. \tag{B5}$$

The last term in the integrand above is fast oscillating for large n, so we will have that for $n > n_{\text{sat}}$

$$\left|\Delta\Gamma_n^{\text{TD}}(\tilde{t})\right| < \epsilon, \tag{B6}$$

where ϵ can be made arbitrarily small.

Let us now consider $\Delta\Gamma_n^{\text{TI}}$. By using Eq. (B4), the relation Eq. (A3), and some tedious but straightforward manipulations, we can rewrite Eq. (B3) as

$$\Delta\Gamma_n^{\text{TI}} = -(-1)^n 4\int_0^\infty \eta(\omega)\cos[\omega(n + 1)\Delta t]d\omega$$

$$+ 4\int_0^\infty \eta(\omega)\frac{(-1)^n\cos\left(\frac{2n+1}{2}\Delta t\omega\right)}{2\cos\left(\frac{\Delta t\omega}{2}\right)}d\omega. \tag{B7}$$

Again, the integrand in the first term above is fast oscillating for large n, while the second term tends to $\Delta\Gamma_\infty$ for $n \to \infty$ [see Eq. (A6)]. We can then write that, for $n > n_{\text{sat}}$,

$$\left|\Delta\Gamma_n^{\text{TI}} - \Delta\Gamma_\infty\right| < \epsilon. \tag{B8}$$

By combining Eqs. (B6) and (B8), we finally obtain that, for *any* $\tilde{t}$ and $n > n_{\text{sat}}$,

$$\Delta\Gamma_n^{\text{PDD}}(\tilde{t}) \approx \Delta\Gamma_\infty. \tag{B9}$$

We note that in the case of a supra-Ohmic environment, by using the fact that $\Gamma_0(\infty) \equiv \lim_{n\to\infty}\Gamma_0(t_{n+1}) = 2\int_0^\infty \eta(\omega)d\omega$

is finite, and using Eqs. (B2) and (B7), we can recast the conditions Eqs. (B6) and (B8) as

$$|\Gamma_0(t > t_{\text{sat}}) - \Gamma_0(\infty)| < \epsilon, \tag{B10}$$

where $t_{\text{sat}} = n_{\text{sat}}\Delta t$. This emphasizes that condition (B9) applies for times at which the natural evolution saturates to its long-term behavior.

APPENDIX C: AVERAGING PROPERTIES OF INTERPOLATED DD SCHEME

We begin by casting the QD Hamiltonian Eq. (1) (with $\alpha = 1/2$) in the following form:

$$H_1 = \sigma_z \otimes B_z + \sigma_0 \otimes B_0, \tag{C1}$$

where B_z and B_0 are operators acting on the phonon bath, and σ_0 and σ_z denote the identity and the Pauli matrix acting on the exciton qubit, respectively. This allows us to express the evolution in the presence of the ith CP cycle by the propagator

$$U_i^{\text{CP}}\left(4\Delta t_i^{\text{CP}}\right) = U_f\left(\Delta t_i^{\text{CP}}\right)XU_f\left(2\Delta t_i^{\text{CP}}\right)XU_f\left(\Delta t_i^{\text{CP}}\right),$$

where $U_f(t) = \exp(-tH_1)$ represents free evolution for a time t. If we define

$$H_2 \equiv -\sigma_z \otimes B_z + \sigma_0 \otimes B_0 = XH_1X, \tag{C2}$$

we can write the entire sequence propagator as a Magnus series expansion [6],

$$U(t) = \exp\sum_{i=1}^\infty A_i(t), \tag{C3}$$

for which, in the limit of sufficiently fast control, we can consider only the first two lowest-order terms in Δt [9]. Specifically (in units where $\hbar = 1$),

$$A_1 = -i\int_0^t dt_1 H(t_1), \tag{C4}$$

$$A_2 = -\frac{1}{2}\int_0^t dt_1 \int_0^{t_1} dt_2[H(t_1), H(t_2)], \tag{C5}$$

where $H(t) = U_{\text{ctrl}}^\dagger(t)HU_{\text{ctrl}}(t)$ is the time-dependent (piecewise constant, for instantaneous pulses) effective Hamiltonian that describes the evolution under the control propagator $U_{\text{ctrl}}(t)$ resulting from the applied pulses [2,5,9].

For the sequence of different CP cycles described in Sec. V, A_1 is proportional to the identity operator, and hence does not contribute to dephasing. This is a simple consequence of the qubit spending equal amounts of time in each of the computational basis states. More interestingly, we find

$$A_2 = \int_0^{t_n^{\text{CP}}+4\Delta t^{\text{CP}}} dt_1 \int_0^{t_1} dt_2[H(t_1), H(t_2)]$$

$$= \sum_{i=1}^n \int_{t_i}^{t_i^{\text{CP}}+4\Delta t^{\text{CP}}} dt_1 \int_0^{t_1} dt_2[H(t_1), H(t_2)]$$

$$= \sum_{i=1}^n \left[\left(\int_{t_i}^{t_i+\Delta t^{\text{CP}}} dt_1 \int_0^{t_1} dt_2 + \int_{t_i+\Delta t^{\text{CP}}}^{t_i+3\Delta t^{\text{CP}}} dt_1 \int_0^{t_1} dt_2 \right.\right.$$

$$\left.\left. + \int_{t_i+3\Delta t^{\text{CP}}}^{t_i+4\Delta t^{\text{CP}}} dt_1 \int_0^{t_1} dt_2\right)[H(t_1), H(t_2)]\right]$$

$$= \sum_{i=1}^{n} \left[\int_{t_i}^{t_i + \Delta t^{CP}} dt_1 \sum_{j=1}^{i-1} 2\Delta t_j^{CP} [H_1, H_2] \right.$$
$$+ \int_{t_i + \Delta t^{CP}}^{t_i + 3\Delta t^{CP}} dt_1 \left(\sum_{j=1}^{i-1} 2\Delta t_j^{CP} + \Delta t_i^{CP} \right) [H_2, H_1]$$
$$\left. + \int_{t_i + 3\Delta t^{CP}}^{t_i + 4\Delta t^{CP}} dt_1 \sum_{j=1}^{i} 2\Delta t_j^{CP} [H_1, H_2] \right]$$

$$= \sum_{i=1}^{n} \left[\Delta t_i^{CP} \sum_{j=1}^{i-1} 2\Delta t_j^{CP} [H_1, H_2] + 2\Delta t_i^{CP} \left(\sum_{j=1}^{i-1} 2\Delta t_j^{CP} \right. \right.$$
$$\left. + \Delta t_i^{CP} \right) [H_2, H_1] + \Delta t_i^{CP} \sum_{j=1}^{i} 2\Delta t_j^{CP} [H_1, H_2] \Bigg]$$
$$= 0,$$

again up to irrelevant pure-bath terms. This confirms the second-order cancellation claimed in the main text.

[1] L. Viola and S. Lloyd, Phys. Rev. A **58**, 2733 (1998).

[2] L. Viola, E. Knill, and S. Lloyd, Phys. Rev. Lett. **82**, 2417 (1999).

[3] E. L. Hahn, Phys. Rev. **80**, 580 (1950).

[4] U. Haeberlen and J. S. Waugh, Phys. Rev. **175**, 453 (1968).

[5] U. Haeberlen, *High Resolution NMR in Solids: Selective Averaging* (Academic Press, New York, 1976); C. P. Slichter, *Principles of Magnetic Resonance* (Springer-Verlag, New York, 1992).

[6] W. Magnus, Commun. Pure Appl. Math. **7**, 649 (1954).

[7] H. Carr and E. Purcell, Phys. Rev. **94**, 630 (1954); S. Meiboom and D. Gill, Rev. Sci. Instrum. **29**, 688 (1958).

[8] K. Khodjasteh and D. A. Lidar, Phys. Rev. Lett. **95**, 180501 (2005).

[9] K. Khodjasteh and D. A. Lidar, Phys. Rev. A **75**, 062310 (2007).

[10] L. Viola and E. Knill, Phys. Rev. Lett. **94**, 060502 (2005).

[11] L. F. Santos and L. Viola, Phys. Rev. A **72**, 062303 (2005); New J. Phys. **10**, 083009 (2008).

[12] D. Dhar, L. K. Grover, and S. M. Roy, Phys. Rev. Lett. **96**, 100405 (2006).

[13] G. S. Uhrig, Phys. Rev. Lett. **98**, 100504 (2007).

[14] G. S. Uhrig, New J. Phys. **10**, 083024 (2008).

[15] S. Pasini and G. S. Uhrig, Phys. Rev. A **81**, 012309 (2010).

[16] B. Lee, W. M. Witzel, and S. Das Sarma, Phys. Rev. Lett. **100**, 160505 (2008).

[17] W. Yang and R.-B. Liu, Phys. Rev. Lett. **101**, 180403 (2008).

[18] M. J. Biercuk, H. Uys, A. P. Van Devender, N. Shiga, W. M. Itano, and J. J. Bollinger, Nature (London) **458**, 996 (2009).

[19] H. Uys, M. J. Biercuk, and J. J. Bollinger, Phys. Rev. Lett. **103**, 040501 (2009).

[20] G. S. Uhrig, Phys. Rev. Lett. **102**, 120502 (2009).

[21] J. R. West, B. H. Fong, and D. A. Lidar, Phys. Rev. Lett. **104**, 130501 (2010).

[22] J. Clausen, G. Bensky, and G. Kurizki, Phys. Rev. Lett. **104**, 040401 (2010).

[23] A (deterministic) DD protocol is *efficient* if the control effort (as quantified, for instance, by the required number of pulses) scales polynomially with the system size (number of qubits) and the order to which the unwanted interaction is suppressed, in a suitably defined perturbative sense (typically, with respect to a Magnus series expansion; see, e.g., Refs. [6,24]).

[24] F. Casas, J. Phys. A **40**, 15001 (2007).

[25] W. M. Witzel and S. Das Sarma, Phys. Rev. B **76**, 241303(R) (2007).

[26] W. Zhang, N. P. Konstantinidis, V. V. Dobrovitski, B. N. Harmon, L. F. Santos, and L. Viola, Phys. Rev. B **77**, 125336 (2008).

[27] L. Faoro and L. Viola, Phys. Rev. Lett. **92**, 117905 (2004).

[28] L. Cywinski, R. M. Lutchyn, C. P. Nave, and S. Das Sarma, Phys. Rev. B **77**, 174509 (2008).

[29] J. R. West, D. A. Lidar, B. H. Fong, M. F. Gyure, X. Peng, and D. Suter, e-print arXiv:0911.2398.

[30] Michael J. Biercuk, Hermann Uys†, Aaron P. VanDevender, Nobuyasu Shiga, Wayne M. Itano, and John J. Bollinger, Phys. Rev. A **79**, 062324 (2009).

[31] J. Du, X. Rong, N. Zhao, Y. Wang, J. Yang, and R. B. Liu, Nature (London) **461**, 1265 (2009).

[32] E. R. Jenista, A. M. Stokes, R. Tamara Branca, and W. Warren, J. Chem. Phys. **131**, 204510 (2009).

[33] E. Biolatti, I. D'Amico, P. Zanardi, and F. Rossi, Phys. Rev. B **65**, 075306 (2002).

[34] See G. Chen, N. H. Bonadeo, D. G. Steel, D. Gammon, D. S. Katzer, D. Park, and L. J. Sham, Science **289**, 1906 (2000); S. De Rinaldis, I. D'Amico, E. Biolatti, R. Rinaldi, R. Cingolani, and F. Rossi, Phys. Rev. B **65**, 081309(R) (2002); X. Li, Y. Wu, D. Steel, D. Gammon, T. H. Stievater, D. S. Katzer, D. Park, C. Piermarocchi, and L. J. Sham, Science **301**, 809 (2003); E. Pazy, E. Biolatti, T. Calarco, I. D'Amico, P. Zanardi, F. Rossi, and P. Zoller, Europhys. Lett. **62**, 175 (2003); M. Feng, I. D'Amico, P. Zanardi, and F. Rossi, *ibid.* **66**, 14 (2004); A. Nazir, B. W. Lovett, S. D. Barrett, T. P. Spiller, and G. A. D. Briggs, Phys. Rev. Lett. **93**, 150502 (2004); T. E. Hodgson, M. F. Bertino, N. Leventis, and I. D'Amico, J. Appl. Phys. **101**, 114319 (2007); T. P. Spiller, I. D'Amico, and B. W. Lovett, New J. Phys. **9**, 20 (2007); A. J. Ramsay, R. S. Kolodka, F. Bello, P. W. Fry, W. K. Ng, A. Tahraoui, H. Y. Liu, M. Hopkinson, D. M. Whittaker, A. M. Fox, and M. S. Skolnick, Phys. Rev. B **75**, 113302 (2007); A. J. Ramsay, S. J. Boyle, R. S. Kolodka, J. B. B. Oliveira, J. Skiba-Szymanska, H. Y. Liu, M. Hopkinson, A. M. Fox, and M. S. Skolnick, Phys. Rev. Lett. **100**, 197401 (2008).

[35] M. Feng, I. D'Amico, P. Zanardi, and F. Rossi, Phys. Rev. A **67**, 014306 (2003).

[36] M. S. Sherwin, A. Imamoglu, and T. Montroy, Phys. Rev. A **60**, 3508 (1999).

[37] B. Krummheuer, V. M. Axt, and T. Kuhn, Phys. Rev. B **65**, 195313 (2002).

[38] T. E. Hodgson, L. Viola, and I. D'Amico, Phys. Rev. B **78**, 165311 (2008).

[39] H. K. Ng, D. A. Lidar, and J. Preskill, e-print arXiv:0911.3202.

[40] Y. Sagi, I. Almog, and N. Davidson, e-print arXiv:0905.0286; e-print arXiv:1004.1011.

[41] Y. Nakamura, Y. A. Pashkin, T. Yamamoto, and J. S. Tsai, Phys. Rev. Lett. **88**, 047901 (2002); F. Yoshihara, K. Harrabi, A. O. Niskanen, Y. Nakamura, and J. S. Tsai, *ibid.* **97**, 167001 (2006); K. Kakuyanagi, T. Meno, S. Saito, H. Nakano, K. Semba, H. Takayanagi, F. Deppe, and A. Shnirman, *ibid.* **98**, 047004 (2007); R. C. Bialczak, R. McDermott, M. Ansmann, M. Hofheinz, N. Katz, E. Lucero, M. Neeley, A. D. O'Connell, H. Wang, A. N. Cleland, and J. M. Martinis, *ibid.* **99**, 187006 (2007); Y. A. Pashkin, O. Astafiev, T. Yamamoto, Y. Nakamura, and J. S. Tsai, Quantum Inf. Process. **8**, 55 (2009).

[42] X. Hu and S. Das Sarma, Phys. Rev. Lett. **96**, 100501 (2006); G. Ramon and X. Hu, Phys. Rev. B **81**, 045304 (2010).

[43] G. M. Palma, K.-A. Suominen, and A. K. Ekert, Proc. R. Soc. London, Ser. A **452**, 567 (1996).

[44] V. Privman and D. Mozyrsky, J. Stat. Phys. **91**, 787 (1998); D. Solenov and V. Privman, Int. J. Mod. Phys. B **20**, 1476 (2006).

[45] C. Uchiyama and M. Aihara, Phys. Rev. A **66**, 032313 (2002).

[46] V. M. Axt, P. Machnikowski, and T. Kuhn, Phys. Rev. B **71**, 155305 (2005).

[47] B. Krummheuer, V. M. Axt, T. Kuhn, I. D'Amico, and F. Rossi, Phys. Rev. B **71**, 235329 (2005).

[48] An important difference between CDD protocols constructed out of two-axis controls (as in Ref. [8]) and single-axis controls (as examined here) stems from the fact that the relevant DD group does not act irreducibly in the latter case. While group reducibility can, in general, worsen CDD performance [11], this is not expected to play a role in purely dephasing settings, since all the higher-order system-bath Magnus terms are proportional to σ_z.

[49] W. Zhang, V. V. Dobrovitski, L. F. Santos, L. Viola, and B. Harmon, J. Mod. Opt. **54**, 2629 (2007).

[50] S. Gheorghiu-Svirschevski, Phys. Rev. A **66**, 032101 (2002).

[51] W. Zhang, V. V. Dobrovitski, L. F. Santos, L. Viola, and B. N. Harmon, Phys. Rev. B **75**, 201302(R) (2007).

[52] W. Zhang and J. Zhuang, Phys. Rev. A **79**, 012310 (2009).

[53] G. Uhrig and D. A. Lidar, e-print arXiv:1002.1484.

[54] L. F. Santos and L. Viola, J. Mod. Opt. **53**, 2559 (2006).

[55] L. Viola and E. Knill, Phys. Rev. Lett. **90**, 037901 (2003).

[56] K. Khodjasteh and L. Viola, Phys. Rev. Lett. **102**, 080501 (2009); K. Khodjasteh, D. A. Lidar, and L. Viola, *ibid.* **104**, 090501 (2010).

[57] K. Khodjasteh and L. Viola, Phys. Rev. A **80**, 032314 (2009).

[58] L. Cywinski, W. M. Witzel, and S. Das Sarma, Phys. Rev. B **79**, 245314 (2009).